

7-10

NACA RM A51L17b

~~53 28 46~~

~~NACA~~



6368

RESEARCH MEMORANDUM

A CORRELATION BY MEANS OF THE TRANSONIC SIMILARITY RULES
OF THE EXPERIMENTALLY DETERMINED CHARACTERISTICS OF
22 RECTANGULAR WINGS OF SYMMETRICAL PROFILE

By John B. McDevitt

Ames Aeronautical Laboratory
Moffett Field, Calif.

Classification cancelled (or changed to Unclassified)
By Authority of NASA Tech Pub. Announcement
(OFFICER AUTHORIZED TO CHANGE)
73 9 Nov 54

By [Signature]
GRADE OF OFFICER MAKING CHANGE)
11A2161
DATE

~~This material contains information affecting the national defense of the United States within the meaning of the espionage laws, the transmission or revelation of which in any manner to an unauthorized person is prohibited by law.~~

NATIONAL ADVISORY COMMITTEE FOR AERONAUTICS

WASHINGTON
February 25, 1952

31998/13

~~CONFIDENTIAL~~

NATIONAL ADVISORY COMMITTEE FOR AERONAUTICS

RESEARCH MEMORANDUM

A CORRELATION BY MEANS OF THE TRANSONIC SIMILARITY RULES
OF THE EXPERIMENTALLY DETERMINED CHARACTERISTICS OF
22 RECTANGULAR WINGS OF SYMMETRICAL PROFILE

By John B. McDevitt

SUMMARY

The transonic similarity rules have been applied to the correlation of experimental data for a series of 22 rectangular wings having symmetrical NACA 63A-series sections, aspect ratios from 1/2 to 6, and thicknesses from 2 to 10 percent. The data were obtained by use of the transonic bump technique over a Mach number range from 0.40 to 1.10, corresponding to a Reynolds number range from 1.25 to 2.05 million. The results show that it is possible to correlate experimental data throughout the subsonic, transonic, and moderate supersonic regimes by using the transonic similarity parameters in forms which are consistent with the Prandtl-Glauert rule of linearized theory.

The multiple families of basic data curves for the various aspect ratios and thickness ratios have been summarized in single presentations involving only one geometric variable - the product of the aspect ratio and the 1/3 power of the thickness ratio.

INTRODUCTION

A unified approach toward an understanding of transonic flows has been achieved only in recent years. Our meager knowledge of transonic flows, in comparison with the more complete and cogent understanding of subsonic and supersonic flows, is due not only to the complexities of the mathematics involved but also to the limitations of test facilities at transonic speeds.

Similarity rules for transonic flow in two dimensions were derived by von Kármán (reference 1) and were extended recently by Spreiter (reference 2) and Berndt (reference 3) to include wings of finite span.

~~CONFIDENTIAL~~

These rules can be shown to coincide with one of the possible forms of the Prandtl-Glauert rule of subsonic and supersonic flows. (Reference 2.) Although the similarity rules do not provide explicit solutions, they do suggest the manner in which experimental data can be correlated.

A recent systematic experimental investigation of the effects of wing aspect ratio and thickness at transonic speeds (reference 4) has provided experimental data ideally suited to correlation using the transonic similarity parameters. The analysis of these data is presented in this paper to provide the transonic characteristics of rectangular wings of symmetrical profile and to help evaluate the usefulness of the transonic similarity parameters for the correlation of experimental data.

The similarity rules are presented in slightly modified forms to permit a direct and convenient application in the data correlation. The form of the data presentation was chosen so that direct comparisons with the various linearized theories could be indicated.

The correlation is applied to the experimental data for 22 rectangular wings having symmetrical NACA 63A-series sections, aspect ratios from 1/2 to 6, and thicknesses from 2 to 10 percent. The data were obtained by use of the transonic bump technique over a Mach number range of 0.40 to 1.10, corresponding to a Reynolds number range from 1.25 to 2.05 million. The basic data for the aspect ratios 1, 2, 4, and 6 have been published in reference 4. The basic data for the aspect ratios 0.5, 1.5, and 3 were obtained by identical testing procedures but have not been published previously. A description of the wing models and the testing procedure is given in reference 4.

SYMBOLS

A	aspect ratio $\left(\frac{b}{c}\right)$
b	wing span
c	wing chord
C_D	total drag coefficient $\left(\frac{\text{total drag}}{qS}\right)$
$C_{D_{\min}}$	minimum drag coefficient
$(C_{D_p})_{\min}$	minimum pressure-drag coefficient
C_{D_f}	friction-drag coefficient, assumed equal to minimum drag coefficient at 0.7 Mach number

ΔC_D	drag coefficient due to lift ($C_D - C_{D_{min}}$)
C_L	lift coefficient $\left(\frac{\text{lift}}{qS}\right)$
$C_{L_{opt}}$	lift coefficient for maximum lift-drag ratio
C_m	pitching-moment coefficient, referred to $0.25c$ $\left(\frac{\text{pitching moment}}{qSc}\right)$
C_p	pressure coefficient
$F\left(\frac{x}{c}, \frac{y}{b}\right)$	ordinate distribution function
$f\left(\frac{x}{c}, \frac{y}{b}\right)$	thickness distribution function
$g\left(\frac{x}{c}, \frac{y}{b}\right)$	camber distribution function
h	camber parameter proportional to the amount of camber
$\left(\frac{L}{D}\right)_{max}$	maximum lift-drag ratio
M	free-stream Mach number
M_{cr}	critical Mach number
M_{DD}	drag-divergence Mach number
q	dynamic pressure
S	wing area
t/c	thickness-to-chord ratio
x, y, z	Cartesian coordinates where x extends in the direction of the free-stream velocity
α	angle of attack
γ	ratio of specific heats (for air $\gamma = 1.4$)
τ	ordinate-amplitude parameter

ϕ	perturbation-velocity potential
$\frac{dC_L}{d\alpha}$, $C_{L\alpha}$	slope of lift curve, measured at zero lift coefficient
$\frac{dC_m}{dC_L}$	slope of pitching-moment curve
D_p	pressure-drag function
ΔD	drag-due-to-lift function
L	lift function
M	pitching-moment function
P	pressure-coefficient function

THEORETICAL CONSIDERATIONS

Transonic Similarity Rules

Similarity rules (references 1, 2, and 3) for the transonic flow around thin wings show how a wing can be affinely distorted in order to retain a related potential distribution when the free-stream Mach number is altered. These rules of correspondence can be shown to coincide with one of the possible forms of the Prandtl-Glauert rule, derived from the linearized potential equation of subsonic or supersonic flows (reference 2). The various results of linearized theory can be expressed in terms of the transonic similarity parameters and the use of these parameters will be consistent for both the linearized theory and the nonlinear transonic theory.

Experience has shown that the linearized potential equation is a good approximation for sufficiently thin wings when the whole field of flow is subsonic or well-established supersonically. In the transonic regime certain nonlinear terms must be retained to show the mixed nature of the flow. The nonlinear terms of the basic potential equation are important only near sonic speed and only the nonlinear terms involving derivatives with respect to the direction of the undisturbed fluid motion need be retained, since perturbations in sonic flow diminish more slowly in the directions perpendicular to the flow than in the direction parallel to it. This assumption is valid only for unswept plan forms, which is the only case to be considered here. The basic potential equation may therefore be written as

$$(1-M^2)\phi_{xx} + \phi_{yy} + \phi_{zz} = (\gamma+1)M^2\phi_x\phi_{xx} \quad (1)$$

where M is the free-stream Mach number and ϕ is the perturbation-velocity potential normalized by division by the free-stream velocity. This equation retains the essential features of both linearized and transonic theory and the similarity rules may be obtained from this equation and applied at subsonic, transonic, and moderately supersonic Mach numbers.

Similarity of flow about wings of finite span requires the constancy of two parameters $(M^2-1)A^2$ and

$$\frac{M^2-1}{\left[\tau \frac{\partial}{\partial(x/c)} F\left(\frac{x}{c}, \frac{y}{b}\right)\right]^{2/3}}$$

where τ is an ordinate-amplitude parameter and $F\left(\frac{x}{c}, \frac{y}{b}\right)$ is the ordinate distribution function. In general, τ may be used to denote changes in profile thickness, angle of attack, and camber. The constancy of these two parameters implies the existence of an alternative similarity parameter

$$A^3 \tau \frac{\partial}{\partial(x/c)} F\left(\frac{x}{c}, \frac{y}{b}\right)$$

which is of fundamental importance. Since the ratio of specific heats γ is constant for a fixed medium the expression $(\gamma+1)$ which appears in equation (1) has not been retained in the similarity parameters nor in the following similarity rules.

The similarity rule for the pressure coefficient on the surface of the wing may be written in the form

$$c_p = \left[\tau \frac{\partial}{\partial(x/c)} F\left(\frac{x}{c}, \frac{y}{b}\right)\right]^{2/3} P \left\{ \frac{M^2-1}{\left[\tau \frac{\partial}{\partial(x/c)} F\left(\frac{x}{c}, \frac{y}{b}\right)\right]^{2/3}}, \right. \\ \left. A \left[\tau \frac{\partial}{\partial(x/c)} F\left(\frac{x}{c}, \frac{y}{b}\right)\right]^{1/3}; \frac{x}{c}, \frac{y}{b} \right\} \quad (2)$$

The expression $\tau \frac{\partial}{\partial(x/c)} F\left(\frac{x}{c}, \frac{y}{b}\right)$ represents the slope of the airfoil surface and can be expressed as

$$\tau \frac{\partial}{\partial(x/c)} F\left(\frac{x}{c}, \frac{y}{b}\right) = (t/c) \frac{\partial}{\partial(x/c)} \left[f\left(\frac{x}{c}, \frac{y}{b}\right) + \frac{h}{t/c} g\left(\frac{x}{c}, \frac{y}{b}\right) - \frac{\alpha}{t/c} \frac{x}{c} \right] \quad (3)$$

where $f\left(\frac{x}{c}, \frac{y}{b}\right)$ and $g\left(\frac{x}{c}, \frac{y}{b}\right)$ are the airfoil thickness and camber distribution functions with the origin at the leading edge of the root chord and the parameter h is proportional to the amount of camber. For airfoils having the same thickness and camber distribution functions the similarity rule for the pressure coefficient may be expressed in the more useful form

$$C_p = (t/c)^{2/3} P \left[\frac{M^2-1}{(t/c)^{2/3}}, A(t/c)^{1/3}, \frac{\alpha}{t/c}, \frac{h}{t/c}, \frac{x}{c}, \frac{y}{b} \right] \quad (4)$$

In this equation α and t/c can be simultaneously interchanged, that is, t/c may be replaced by α , and α by t/c . This is possible by virtue of the presence of the parameter $\frac{\alpha}{t/c}$. The form of the function P , however, may be altered in the process.

Generalized Force and Moment Coefficients

From the similarity rule for the pressure coefficient the generalized expressions for lift coefficient and lift-curve slope are obtained

$$\frac{C_L}{\alpha^{2/3}} = L \left[\frac{M^2-1}{(t/c)^{2/3}}, A(t/c)^{1/3}, \frac{\alpha}{t/c}, \frac{h}{t/c} \right] \quad (5)$$

and

$$(t/c)^{1/3} \frac{dC_L}{d\alpha} = L_1 \left[\frac{M^2-1}{(t/c)^{2/3}}, A(t/c)^{1/3}, \frac{\alpha}{t/c}, \frac{h}{t/c} \right] \quad (6)$$

When the lift coefficient varies linearly with angle of attack the parameter $\frac{\alpha}{t/c}$ may be omitted from equation (6).

The generalized expressions for moment coefficient, pitching-moment slope, and center of pressure are

$$\frac{C_m}{\alpha^{2/3}} = M \left[\frac{M^2-1}{(t/c)^{2/3}}, A(t/c)^{1/3}, \frac{\alpha}{t/c}, \frac{h}{t/c} \right] \quad (7)$$

$$\frac{dC_m}{dC_L} = M_1 \left[\frac{M^2-1}{(t/c)^{2/3}}, A(t/c)^{1/3}, \frac{\alpha}{t/c}, \frac{h}{t/c} \right] \quad (8)$$

$$C.P. = M_2 \left[\frac{M^2-1}{(t/c)^{2/3}}, A(t/c)^{1/3}, \frac{\alpha}{t/c}, \frac{h}{t/c} \right] \quad (9)$$

The total drag coefficient may be expressed as

$$C_D = C_{Df} + (C_{Dp})_{\min} + \Delta C_D \quad (10)$$

The friction-drag coefficient C_{Df} cannot be expressed in terms of the similarity parameters since the theory neglects all viscous effects. The generalized expression for minimum pressure drag is

$$\frac{(C_{Dp})_{\min}}{(t/c)^{5/3}} = D_p \left[\frac{M^2-1}{(t/c)^{2/3}}, A(t/c)^{1/3}, \frac{h}{t/c} \right] \quad (11)$$

Although the similarity rule implies a generalized drag-due-to-lift parameter $\frac{\Delta C_D}{\alpha^{5/3}}$, a more useful generalized expression is

$$(t/c)^{1/3} \frac{\Delta C_D}{\alpha^2} = \Delta D_1 \left[\frac{M^2-1}{(t/c)^{2/3}}, A(t/c)^{1/3}, \frac{\alpha}{t/c}, \frac{h}{t/c} \right] \quad (12)$$

and a comparison of ΔC_D with C_L^2 may be obtained from

$$(t/c)^{-1/3} \frac{\Delta C_D}{C_L^2} = \Delta D_2 \left[\frac{M^2-1}{(t/c)^{2/3}}, A(t/c)^{1/3}, \frac{\alpha}{t/c}, \frac{h}{t/c} \right] \quad (13)$$

In equations (12) and (13) the ratio $\frac{\alpha}{t/c}$ may be neglected if the drag due to lift shows a parabolic variation with angle of attack and with lift coefficient.

A comparison of drag due to lift with the limits for drag with full leading-edge suction (elliptic spanwise loading) and drag with no leading-edge suction may be obtained by use of the expression

$$\frac{C_L^2}{\pi A} \leq \Delta C_D \leq C_L \alpha$$

or, when written in terms of the generalized lift-curve slope and assuming a linear variation of C_L with α ,

$$\frac{[(t/c)^{1/3} C_{L\alpha}]^2}{\pi A (t/c)^{1/3}} \leq (t/c)^{1/3} \frac{\Delta C_D}{\alpha^2} \leq (t/c)^{1/3} C_{L\alpha} \quad (14)$$

In the preceding generalized expressions the argument $\frac{h}{t/c}$ vanishes for symmetrical profiles, $\frac{M^2-1}{(t/c)^{2/3}}$ vanishes at $M = 1$, and in the case of two-dimensional flow $A(t/c)^{1/3}$ does not enter into the similarity rules.

~~CONFIDENTIAL~~

Use of the Similarity Parameters

The generalized coefficients and derivatives can be applied only to experimental data for wings having the same thickness and camber distribution functions. For constant values of $\frac{\alpha}{t/c}$ and $\frac{h}{t/c}$ the generalized expressions will remain constant and the flow patterns will be similar if the Mach numbers are chosen so that $\sqrt{|M^2-1|}A$ and $\frac{M^2-1}{(t/c)^{2/3}}$ remain constant. This will be possible only if the wings have equal values $A(t/c)^{1/3}$, and thus similarity can exist only if the wing geometries are related in a special manner. The variations of Mach number with thickness ratio and with aspect ratio for several constant values of $\sqrt{|M^2-1|}A$ and $\frac{M^2-1}{(t/c)^{2/3}}$ are shown in figure 1(a). The variations between aspect ratio and thickness ratio for several constant values of $A(t/c)^{1/3}$ are shown in figure 1(b).

According to small perturbation theory the thickness ratio must be small but no restriction is necessary concerning the magnitude of the aspect ratio. A given value of $A(t/c)^{1/3}$ must always correspond to a small thickness ratio and therefore a systematic survey of airfoil data should cover a wide range of $A(t/c)^{1/3}$ values as was done for the analysis of this paper. (The values of $A(t/c)^{1/3}$ for these airfoils are tabulated in table I.)

For wings having unequal values of $A(t/c)^{1/3}$ the use of the two parameters $\frac{M^2-1}{(t/c)^{2/3}}$ and $A(t/c)^{1/3}$ suggests two different but essentially equivalent forms of data correlation, one showing the variation of the generalized coefficients with $A(t/c)^{1/3}$ for constant values of the speed parameter $\frac{M^2-1}{(t/c)^{2/3}}$, the other showing the variation with $\frac{M^2-1}{(t/c)^{2/3}}$ for constant values of $A(t/c)^{1/3}$. For convenience, the correlation in this paper will be made for constant values of $\frac{M^2-1}{(t/c)^{2/3}}$ and the results summarized for constant values of $A(t/c)^{1/3}$. Thus, the use of the similarity parameters permits the multiple families of basic data curves for various aspect ratios and thickness ratios to be summarized in a presentation involving only one geometric variable, the parameter $A(t/c)^{1/3}$.

The actual flow about wings will always violate to some extent the assumptions necessary in the derivation of small disturbance theory, which assumes that the flow deflection is everywhere small. The theory also ignores the existence of a stagnation region at the leading edge

and of a boundary layer. A theory for transonic flow must also consider the extent and position of the mixed subsonic and supersonic flow regions. Although the essential properties of shock waves and of Prandtl-Meyer flow can be approximated in terms of the speed parameter, provided the flow deflection angle is small (references 1 and 5), a successful correlation of experimental data will be possible only if the boundaries of the mixed flow regions for related airfoils possess similitude of size and position.

The usefulness of the similarity rules can be determined only from a systematic survey of experimental data.

Slender-Wing Theory

A solution in general is not known for the nonlinear transonic potential equation

$$(1-M^2)\phi_{xx} + \phi_{yy} + \phi_{zz} = (\gamma+1)M^2\phi_x\phi_{xx} \quad (1)$$

For two-dimensional flow the partial derivatives ϕ_x and ϕ_{xx} are known to become very large as the Mach number approaches 1. However, for wings of slender plan form, that is, wings of sufficiently low aspect ratio, these derivatives may be considered to be of the same relative magnitude as the partial derivatives ϕ_{yy} and ϕ_{zz} and the nonlinear term $(\gamma+1)M^2\phi_x\phi_{xx}$, which is of the second order, can therefore be neglected. Thus, for slender wings the linearized equation

$$(1-M^2)\phi_{xx} + \phi_{yy} + \phi_{zz} = 0 \quad (15)$$

can be used throughout the transonic speed range.

For vanishingly small aspect ratios, or for moderate aspect ratios at near sonic speeds where the coefficient $1-M^2$ becomes small independently of ϕ_{xx} , the linearized equation reduces to Laplace's equation in two dimensions

$$\phi_{yy} + \phi_{zz} = 0$$

for which solutions are well known. Such solutions have been given by R. T. Jones (reference 6) for the case of slender, pointed wings and by various authors (see, e.g., references 7 and 8) for slender wing-body combinations. The slender-wing theory furnishes the interesting result that all the lift is carried upstream of the point of maximum span and the center of pressure of a rectangular wing of vanishing aspect ratio will, at sonic speed, be at the leading edge. The theory, however, is unable to predict the effects of profile thickness and is restricted to

the lifting case. A solution cannot be obtained for the zero-lift pressure drag.

The theory of reference 6 provides the following expressions for the lift and drag coefficients:

$$C_L = \frac{\pi}{2} A\alpha$$

$$\Delta C_D = \frac{\pi}{4} A\alpha^2 \quad (\text{full leading-edge suction})$$

The alternative expressions

$$(t/c)^{1/3} \frac{dC_L}{d\alpha} = \frac{\pi}{2} A(t/c)^{1/3} \quad (16)$$

$$(t/c)^{1/3} \frac{\Delta C_D}{\alpha^2} = \frac{\pi}{4} A(t/c)^{1/3} \quad (\text{full leading-edge suction}) \quad (17)$$

will be used in the data correlation to obtain a comparison between theory and experiment for the wings of low aspect ratio at the sonic Mach number.

DATA CORRELATION

Before beginning the data correlation it might be well to point out that the experimental data were obtained by mounting semispan wing models in the high-velocity flow field of the Ames 16-foot high-speed wind-tunnel transonic bump. The streamlines of the bump flow field are slightly curved with Mach number gradients in the plane of the wing model. Typical Mach number contours are presented in reference 4. These gradients are most pronounced at the higher Mach numbers and for the larger aspect ratios. The effects of the nonuniformity of the flow field are unknown but a certain rounding off of any sharp breaks in force and moment coefficient variation with Mach number can be expected.

Minimum Pressure Drag

The drag-similarity rule cannot be applied directly to a correlation of minimum drag data since small perturbation theory ignores the existence of friction drag. The friction drag coefficient is believed to change little with Mach number in the transonic range and the correlation can be applied to the minimum pressure drag coefficient. The minimum pressure drag has been calculated by subtracting a constant friction drag, assumed equal to the minimum drag at 0.7 Mach number, from the minimum drag, that is,

$$(C_{Dp})_{\min} = C_{D\min} - (C_{D\min})_{M=0.7} \quad (18)$$

The basic data curves for the variation of minimum drag coefficient with Mach number are presented in figure 2. The variation of the generalized coefficient $\frac{(C_{Dp})_{\min}}{(t/c)^{5/3}}$ with the speed parameter $\frac{M^2-1}{(t/c)^{2/3}}$ is shown in figure 3 as an introductory step to the completely generalized data correlation of figures 4 and 5. (The symbols used in fig. 3 represent the actual test data points and were included to show the manner in which the data have been faired.)

The data curves for the wings of aspect ratio 6 in figure 3 may be closely represented by a common curve, indicating that at this aspect ratio the values of $\frac{(C_{Dp})_{\min}}{(t/c)^{5/3}}$ may be considered to depend only on the value of $\frac{M^2-1}{(t/c)^{2/3}}$ and that the flow is essentially two-dimensional.

The aspect-ratio-6 wings also exhibit the negative variation of the force coefficient with Mach number which is characteristic of two-dimensional flows at sonic speed. This variation is a consequence of the relative variations of local and free-stream dynamic pressures. The local Mach numbers are effectively frozen at near-sonic values as the free-stream Mach number increases through the transonic speed range. (See references 9 and 10.) It is interesting to note that the experimental values of $\left(\frac{dC_D}{dM}\right)_{M=1}$ for the wings of aspect ratio 6, figure 2, agree qualitatively with the values implied by the following relationship (an exact theoretical result applicable to symmetrical profiles of any shape, reference 10):

$$\left(\frac{dC_D}{dM}\right)_{M=1} = -\frac{2}{\gamma+1} (C_D)_{M=1} \quad (19)$$

This agreement occurred in spite of the fact that the test conditions are not ideal and do not agree with the concept of an infinite and uniform flow field assumed in the theoretical reasoning.

The lower aspect ratios show increasing effects of three-dimensional flow and the smaller thickness ratios have progressively lower generalized drag coefficients with the exception of the thinnest (2-percent-thick) wing models. These thinnest airfoils have unusually large values of $\frac{(C_{Dp})_{\min}}{(t/c)^{5/3}}$, which are believed to be largely the result of the boundary layer creating an effective thickness considerably larger than the actual profile thickness. The generalized drag coefficients are then magnified for the thin airfoils by the 5/3 powers of the ratios of effective thickness to profile thickness.

The completely generalized correlation of minimum pressure drag is presented in figures 4 and 5. (The symbols used in these figures and in the remaining figures of the report represent values taken from faired curves of preliminary cross plots. A different symbol has been used to represent the data for each particular wing tested.) The transonic correlation for constant values of $\sqrt{|1-M^2|}A$ is presented in figure 4 merely to illustrate the inability of presenting data at the sonic velocity using simultaneously the parameters $\sqrt{|M^2-1|}A$ and $\frac{M^2-1}{(t/c)^{2/3}}$.

The correlation for constant values of $\frac{M^2-1}{(t/c)^{2/3}}$ is presented in figure 5. The correlation is best at the sonic velocity and the curve for this particularly interesting Mach number is repeated in figure 6. Although the data for 2-percent thickness have been omitted from the preceding correlation because the extraordinarily large values interfere with the adjacent correlation curves, these data have been included in figure 6 to show the pronounced effect of the boundary layer for these thinnest profiles.

At the sonic speed the minimum pressure drag is seen to vary linearly with aspect ratio and with the second power of the thickness ratio for values of $A(t/c)^{1/3}$ less than about 1 as can be expressed by

$$(C_{Dp})_{\min} = 2.3A(t/c)^2; \quad M = 1 \quad (20)$$

$$A(t/c)^{1/3} < 1$$

For values of $A(t/c)^{1/3}$ greater than about 1 the generalized coefficient $\frac{(C_{Dp})_{\min}}{(t/c)^{5/3}}$ approaches rapidly and asymptotically toward a constant value for which the minimum pressure drag varies with the 5/3 power of the thickness ratio in accordance with the drag similarity rule for sonic, two-dimensional flow. The extrapolated two-dimensional-flow value for $M=1$, $(C_{Dp})_{\min} = 3.55 (t/c)^{5/3}$, was obtained by plotting against the inverse parameter $1/A(t/c)^{1/3}$. The calculated theoretical pressure drag for a double-wedge profile (reference 11) is somewhat higher.

The correlation of minimum pressure drag is summarized in figure 7 by cross plotting from the faired curves of figure 5. The predicted critical Mach numbers¹ for NACA 630XX profiles are given in reference 13 and may be approximated by $\frac{M_{cr}^2-1}{(t/c)^{2/3}} = -1.95$. The compressibility drag

¹In reference 12 Kaplan has shown that the section critical Mach number, according to first-order linearized theory, is related to the thickness ratio by a constant value of the speed parameter, the constant depending on the particular profile shape.

rise becomes noticeable at slightly higher Mach numbers, that is, for $\frac{M^2-1}{(t/c)^{2/3}} = -1.80$.

The fundamental importance of the similarity parameter $A(t/c)^{1/3}$ is clearly evident from the summarization of minimum pressure drag as presented in figure 7. The curves of figure 1 and the values of table II may be used with figure 7 for convenience in calculating the minimum pressure drag for given values of aspect ratio, thickness ratio, and Mach number.

Lift

The variation of the lift coefficient with angle of attack is essentially linear at moderate angles of attack throughout the Mach number range for aspect ratios greater than 1.5. The lower aspect ratios, however, show an increasingly nonlinear variation of lift with angle of attack and approach the theoretical $\sin^2 \alpha$ variation for vanishing aspect ratio. For convenience the lift analysis will be restricted to a consideration of the lift-curve slope evaluated at zero-lift coefficient, which provides a close approximation for lift characteristics at the moderate angles of attack for which the similarity rules can be expected to hold.

The variation of lift-curve slope with Mach number is shown in figure 8 and is compared with the theoretical lift-curve slopes calculated by applying the three-dimensional Prandtl-Glauert transformation to the Weissinger lifting-line theory of reference 14. The agreement between theory and experiment for aspect ratios greater than about 3 is satisfactory only in the subcritical Mach number range.

Above the critical Mach number an abrupt decrease in lift-curve slope occurs for some of the wings of larger aspect ratio and thickness ratio and is believed to be the result of the formation of strong velocity discontinuities and flow separation at the airfoil surfaces. This "bucket" type variation in the lift-curve slope is a phenomenon apparently dependent on a combination of thickness and aspect-ratio effect since the smaller thickness ratios and smaller aspect ratios show no such irregularities in the lift-curve variation with Mach number. Indeed, it will be shown in the following data correlation that this erratic variation occurs only for the wings having values of $A(t/c)^{1/3}$ greater than about 1.6.

The variation of the generalized lift-curve-slope parameter $(t/c)^{1/3} \left(\frac{dC_L}{d\alpha} \right)_{\alpha=0}$ with the speed parameter $\frac{M^2-1}{(t/c)^{2/3}}$ is shown in

figure 9 as an introductory step to the completely generalized data correlation of figure 10. A comparison of figures 8 and 9 shows that the curves for aspect ratio 6 have converged toward a single variation at the transonic speeds, indicating that the flow is essentially two-dimensional for the higher aspect ratios. For these wings the lift-curve slope shows the characteristic negative variation with Mach number at near-sonic speeds.

The correlation of $(t/c)^{1/3} \left(\frac{dC_L}{d\alpha} \right)_{\alpha=0}$ for several constant values of $\frac{M^2-1}{(t/c)^{2/3}}$ is presented in figure 10. The correlation and comparison with theory are good for the large negative values of the speed parameter (i.e., low Mach numbers) and a reasonably good correlation is indicated at near-sonic speeds. At supercritical Mach numbers and values of $A(t/c)^{1/3}$ greater than 1.6 the poor correlation suggests a separated flow for which the concepts of small perturbation theory would be violated. The value $A(t/c)^{1/3} = 1.6$ appears to be the limiting value for airfoils which do not exhibit noticeable irregularities in lift-curve-slope variation with Mach number.

At $M=1$, and for small values of $A(t/c)^{1/3}$, the experimental lift agrees well with the lifting-line and slender-wing theories. Hence, within the indicated limits, the lift may be approximated by the following equation:

$$C_L = \frac{\pi}{2} A\alpha, \quad M = 1 \quad (21)$$

$$A(t/c)^{1/3} < 1$$

For increasingly greater values of $A(t/c)^{1/3}$ a rapid and apparently asymptotic approach of $(t/c)^{1/3} \left(\frac{dC_L}{d\alpha} \right)_{\alpha=0}$ to a constant value is indicated. The theoretical result of Guderley and Yoshihara² for a double-wedge profile in sonic, two-dimensional flow is included in figure 10.

The results of the data correlation for lift-curve slope are summarized in figure 11 for those values of $A(t/c)^{1/3}$ and $\frac{M^2-1}{(t/c)^{2/3}}$ where a good correlation was indicated.

²This theoretical value of the lift-curve slope was calculated in Air Force Technical Report 6683, Unsymmetric Flow Patterns at Mach Number One, by Gottfried Guderley and Hideo Yoshihara.

Moment

The variation of the degree of static longitudinal stability with Mach number is presented in figure 12. The pitching-moment-curve slope dC_m/dC_L was measured for $\frac{\alpha}{t/c}$ ratios of 0, 1, and 2 radians. (The values of α in degrees are tabulated in table III.)

For the larger aspect ratios $\frac{dC_m}{dC_L}$ varies smoothly with Mach number in the low subsonic and in the supersonic regimes, although at different levels, but behaves erratically at high subsonic speeds. This erratic behavior is probably due to the same causes as the irregularities of the lift-curve slope at the corresponding Mach numbers. At Mach numbers up to the critical the effects of compressibility are relatively small as is predicted by linearized theory. At transonic speeds a large change in the center of pressure occurs for the wings of large aspect ratio as the aerodynamic center moves from the vicinity of the 25-percent-chord point of subsonic speeds towards the 40-percent-chord point. Only for very low values of the aspect ratio is this undesirable change in center of pressure substantially decreased.

The correlation of pitching-moment-curve slope $\frac{dC_m}{dC_L}$ for various values of the speed parameter $\frac{M^2-1}{(t/c)^{2/3}}$ is presented in figure 13. Although considerable scatter of data is evident the curves have been faired favoring the data for the thickness ratio of 4 percent which do show a good correlation. The values of $\frac{dC_m}{dC_L}$ for $\frac{\alpha}{t/c} = 0$ represent the position of the center of pressure and for all values of the speed parameter the center of pressure is shown to move progressively toward the leading edge as the aspect ratio becomes small. At transonic speeds the stability derivative varies almost linearly with $A(t/c)^{1/3}$ for values of $A(t/c)^{1/3}$ less than about 1 with the center of pressure located at the leading edge for vanishing aspect ratio at zero angle of attack. For values of $A(t/c)^{1/3}$ greater than about 1 the stability derivatives may be considered constant and independent of both aspect ratio and thickness ratio.

The pitching-moment-curve slope correlation is summarized in figure 14. When using these curves to estimate $\frac{dC_m}{dC_L}$ for particular values of aspect ratio and thickness ratio the lift coefficient corresponding to a given value of $\frac{\alpha}{t/c}$ can be approximated by use of the identity

$$C_L = (t/c)^{2/3} \left[(t/c)^{1/3} C_{L\alpha} \right] \frac{\alpha}{t/c}$$

In this equation the lift variation with angle of attack has been assumed to be linear. Numerical values for $(t/c)^{1/3} C_{L\alpha}$ can be obtained from the summary curves of figure 11.

Drag Due to Lift

Equation (12) will be used for the correlation of the drag-due-to-lift coefficient ΔC_D . The correlation will be made for several constant values of $\frac{\alpha}{t/c}$ (α in radians), since it is not always known beforehand if it is possible to represent closely the drag due to lift by a parabolic variation with the angle of attack.

The variation of $(t/c)^{1/3} \frac{\Delta C_D}{\alpha^2}$ with the speed parameter $\frac{M^2-1}{(t/c)^{2/3}}$

for the various thickness ratios and aspect ratios is shown in figure 15. The approximate limits for drag with full leading-edge suction (elliptic spanwise loading) and drag with no leading-edge suction as given by equation (14) have been evaluated using the summary curves of figure 11 for the lift-curve slope and are presented in figure 15 to show the degree of leading-edge suction. At transonic speeds the drag force for the larger aspect ratios and thickness ratios is actually somewhat higher than the value corresponding to a resultant force perpendicular to the plane of the wing, suggesting that some increase in separation and viscous effects occurs with increasing angle of attack.

The correlation of $(t/c)^{1/3} \frac{\Delta C_D}{\alpha^2}$ for several constant values of $\frac{M^2-1}{(t/c)^{2/3}}$ and $\frac{\alpha}{t/c}$ is presented in figure 16. The correlation curves for constant $\frac{\alpha}{t/c}$ are presented in the left-hand side and summarized in the right-hand side of figure 16. A poor correlation is indicated for large values of $A(t/c)^{1/3}$ at the large negative values of the speed parameter where the degree of leading-edge suction apparently is changing rapidly with Mach number. When the resultant force becomes normal to the chord line the drag-due-to-lift correlation is connected intimately with the lift correlation. For transonic values of the speed parameter a reasonably good correlation of $(t/c)^{1/3} \frac{\Delta C_D}{\alpha^2}$ is indicated and the various $\frac{\alpha}{t/c}$ curves may be closely represented by a common curve as they should for a parabolic variation of ΔC_D with α .

The sonic data are presented in figure 16(c) and are compared with the low-aspect-ratio theory for both $\Delta C_D = \frac{C_L^2}{\pi A}$ and $\Delta C_D = C_L \alpha$ (where the lift coefficient is given by $C_L = \frac{\pi}{2} A \alpha$). These summary curves show

that the drag due to lift, for low-aspect ratios, is given approximately by

$$\Delta C_D = \frac{\pi}{2} A \alpha^2; \quad M = 1 \quad (22)$$

$$0.5 < A(t/c)^{1/3} < 1.3$$

Only for very low values of $A(t/c)^{1/3}$ does the drag due to lift tend toward the formal result of low-aspect-ratio theory, $\Delta C_D = \frac{\pi}{4} A \alpha^2$.

The drag-due-to-lift correlation is summarized in figure 17. Since the correlation curves were found to be nearly independent of $\frac{\alpha}{t/c}$, especially in the transonic speed range and for the moderate angles of attack used, the presentation is made only for the ratio $\frac{\alpha}{t/c} = 1$.

A comparison of the induced drag for constant lift coefficient may be obtained from a consideration of the generalized parameter $(t/c)^{1/3} \frac{\Delta C_D}{C_L^2}$. The variation of this parameter with $\frac{M^2-1}{(t/c)^{2/3}}$ for constant values of $A(t/c)^{1/3}$ is shown in figure 18 as derived from the lift and drag summary curves of figures 11 and 17. A consistently decreasing drag due to lift, for constant lift coefficient, is indicated for increasing aspect ratio. It should be remembered, however, that the correlation of data does not apply at the high subsonic Mach numbers for values of $A(t/c)^{1/3}$ greater than 1.6. For these wings, of large aspect ratio and large thickness ratio, a reversed and erratic trend of large induced drag results, probably from the large effects of shock-induced flow separation.

ADDITIONAL CONSIDERATIONS

Maximum Lift-Drag Ratio and Optimum Lift Coefficient

The variation of the maximum lift-drag ratio and the corresponding optimum lift coefficient with Mach number is shown in figures 19 and 20.

The maximum lift-drag ratio is expressed by the familiar formula

$$\left(\frac{L}{D}\right)_{\max} = \frac{1}{2} \sqrt{\frac{1}{[C_{Df} + (C_{Dp})_{\min}] \frac{\Delta C_D}{C_L^2}}} \quad (23)$$

provided the variation of ΔC_D with C_L is parabolic. The value of the the friction coefficient C_{Df} for the conditions under consideration may be taken to be 0.006. From the equivalent expression

$$\left(\frac{L}{D}\right)_{\max} = \frac{1}{2(t/c)} \sqrt{\frac{1}{\left[\frac{C_{Df}}{(t/c)^{5/3}} + \frac{(C_{Dp})_{\min}}{(t/c)^{5/3}}\right] (t/c)^{-1/3} \frac{\Delta C_D}{C_L^2}}} \quad (24)$$

it is apparent that the inclusion of the friction drag does not permit a generalized expression for $\left(\frac{L}{D}\right)_{\max}$ in terms of the similarity parameters. A correlation of data must consider, individually, each separate value of the thickness ratio. Although no generalized correlation appears possible a few remarks will be made concerning the effects of aspect ratio and thickness ratio at transonic speeds.

At low speeds and large Reynolds numbers, the maximum lift-drag ratio shows a dependence principally on the value of the aspect ratio. Above the critical Mach number, where the minimum pressure drag becomes large, the lift-drag ratios are found to be essentially independent of the aspect ratio but indicate a pronounced dependence on the thickness ratio. This independence of aspect ratio at transonic speeds is illustrated by the sonic data in figure 21 where the variation with $A(t/c)^{1/3}$ of the two expressions

$$\left[\frac{C_{Df}}{(t/c)^{5/3}}\right] \left[\frac{\Delta C_D}{C_L^2} (t/c)^{-1/3}\right] \quad \text{and} \quad \left[\frac{(C_{Dp})_{\min}}{(t/c)^{5/3}}\right] \left[\frac{\Delta C_D}{C_L^2} (t/c)^{-1/3}\right]$$

used in equation (23) for $\left(\frac{L}{D}\right)_{\max}$, is shown for several thickness ratios. The two variations have a compensating effect that leads to a maximum lift-drag ratio essentially independent of aspect ratio.

The optimum lift coefficient is represented by the following formula when the drag polars are parabolic:

$$C_{Lopt} = \sqrt{\frac{C_{Df} + (C_{Dp})_{\min}}{\frac{\Delta C_D}{C_L^2}}} \quad (25)$$

The basic data curves of figure 20 show that the value of C_{Lopt} at near-sonic speeds decreases with both decreasing aspect ratio and decreasing thickness ratio.

The linear variation of the force coefficients with aspect ratio at the sonic speed is characteristic of the wings having values of $A(t/c)^{1/3}$ less than about 1. The following empirical formulas were obtained by substituting equations (20), (21), and (22) into equations (23) and (25)

$$\left(\frac{L}{D}\right)_{\max} = \frac{1}{2} \sqrt{\frac{\pi/2}{\frac{C_{Df}}{A} + 2.3(t/c)^2}} \quad \left. \begin{array}{l} M = 1 \\ A(t/c)^{1/3} < 1 \end{array} \right\} \quad (26)$$

$$C_{Lopt} = A \sqrt{\pi/2 \left[\frac{C_{Df}}{A} + 2.3(t/c)^2 \right]}$$

The friction drag coefficient may be closely approximated by 0.006 and the calculated values from these formulas agree closely with the sonic experimental data for the aspect-ratio range of 3 to 1.

Drag-Divergence Mach Number

The drag-divergence Mach number M_{DD} may be defined as the Mach number at which a definite and abrupt increase in drag coefficient occurs and is usually chosen as the Mach number for which the rate of change of drag coefficient with Mach number reaches some arbitrary value, say 0.1. A new definition for drag-divergence Mach number follows from a consideration of the similarity rule for the drag coefficient

$$C_D = (t/c)^{5/3} D \left[\frac{M^2-1}{(t/c)^{2/3}}, A(t/c)^{1/3}, \frac{\alpha}{t/c}, \frac{h}{t/c} \right]$$

Differentiating with respect to the Mach number gives

$$\frac{dC_D}{dM} = (t/c)M D_1 \left[\frac{M^2-1}{(t/c)^{2/3}}, A(t/c)^{1/3}, \frac{\alpha}{t/c}, \frac{h}{t/c} \right]$$

The drag-divergence Mach number may now be defined as the Mach number for which

$$\frac{\frac{dC_D}{dM}}{(t/c)M} = \text{constant} \quad (27)$$

and this implies the functional relationship

$$\frac{1-M_{DD}^2}{(t/c)^{2/3}} = f \left[A(t/c)^{1/3}, \frac{\alpha}{t/c}, \frac{h}{t/c} \right] \quad (28)$$

For two-dimensional flows it follows immediately that the relationship between drag-divergence Mach number and thickness ratio for symmetrical wings at zero angle of attack is given by a constant value of $\frac{1-M_{DD}^2}{(t/c)^{2/3}}$.

The experimental drag-divergence Mach numbers for zero lift coefficient $\left(\frac{\alpha}{t/c} = 0\right)$ are correlated in figure 22. For convenience the evaluation has been made for $\frac{dC_D/dM}{(t/c)M} = 1$. According to figure 22 the two-dimensional-flow value for M_{DD} is given approximately by $\frac{1-M_{DD}^2}{(t/c)^{2/3}} = 1.75$ as is indicated by the asymptotic nature of the curve.

CONCLUDING REMARKS

The similarity rules have been used to correlate the experimental data for a series of 22 rectangular, symmetrical wings having NACA 63A0XX sections, aspect ratios from 1/2 to 6, and thicknesses from 2 to 10 percent. The data were obtained by use of the transonic bump technique for a Mach number range of 0.40 to 1.10 and Reynolds number range of 1.25 to 2.05 million.

The results of the correlation have shown that, with the exception of wings having large values of $A(t/c)^{1/3}$ at high subsonic Mach numbers where an erratic variation of the force and moment coefficients with Mach number was indicated, it is possible to correlate experimental data throughout the Mach number range using the transonic similarity parameters. The use of the generalized coefficients has permitted the presentation of experimental data for a wide range of aspect ratios and thickness ratios by a unified method throughout the Mach number range, and the form of presentation used has permitted a direct comparison of the data with the known results of theory.

At the sonic Mach number a linear variation of the force and moment coefficients with aspect ratio was found to be a universal property for wings having values of $A(t/c)^{1/3}$ less than about 1. For increasing values of $A(t/c)^{1/3}$ greater than 1 the generalized coefficients at the sonic speed show a rapid and asymptotic approach to constant values, indicating that a transition from three-dimensional-flow characteristics (where the force and moment coefficients vary linearly with aspect ratio) to two-dimensional-flow characteristics (where the force and moment coefficients are essentially independent of the aspect ratio) occurs near the particular value of $A(t/c)^{1/3}$ equal to 1.

The data correlation was summarized in presentations involving only one geometric variable $A(t/c)^{1/3}$. The summary curves may be used as design charts for estimating the transonic characteristics of rectangular wings provided the airfoil profile does not differ greatly from the NACA 63A series. Although a correlation of experimental data was not possible for the maximum lift-drag ratio and the optimum lift coefficient,

the summary curves for minimum pressure drag and drag due to lift may be used to estimate these values.

Ames Aeronautical Laboratory,
National Advisory Committee for Aeronautics,
Moffett Field, Calif.

REFERENCES

1. von Kármán, Theodore: The Similarity Law of Transonic Flow. Jour. Math. and Physics, vol. XXVI, no. 3, Oct. 1947, pp. 182-190.
2. Spreiter, John R.: Similarity Laws for Transonic Flow About Wings of Finite Span. NACA TN 2273, 1951.
3. Berndt, Sune B.: Similarity Laws for Transonic Flow Around Wings of Finite Aspect Ratio. KTH, Royal Institute of Technology, Tech. Note 14, Stockholm, Sweden, 1950.
4. Nelson, Warren H., and McDevitt, John B.: The Transonic Characteristics of 17 Rectangular, Symmetrical Wing Models of Varying Aspect Ratio and Thickness. NACA RM A51A12, 1951.
5. Oswatitsch, K.: A New Law of Similarity for Profiles Valid in the Transonic Region. TN No. 1902, R.A.E. (British), 1947.
6. Jones, Robert T.: Properties of Low-Aspect-Ratio Pointed Wings at Speeds Below and Above the Speed of Sound. NACA Rep. 835, 1946. (Formerly NACA TN 1032)
7. Lagerstrom, P. A., and Graham, M. E.: Remarks on Low-Aspect-Ratio Configurations in Supersonic Flow. Jour. Aero. Sci., vol. 18, no. 2, Feb. 1951, pp. 91-97.
8. Spreiter, John R.: Aerodynamic Properties of Slender Wing-Body Combinations at Subsonic, Transonic, and Supersonic Speeds. NACA Rep. 962, 1950. (Formerly NACA TN 1662)
9. Liepmann, H. W., and Bryson, A. E., Jr.: Transonic Flow Past Wedge Sections. Jour. Aero. Sci., vol. 17, no. 12, Dec. 1950, pp. 745-755.
10. Vincenti, Walter G., and Wagoner, Cleo B.: Transonic Flow Past a Wedge Profile With Detached Bow Wave - General Analytical Method and Final Calculated Results. NACA TN 2339, 1951.
11. Guderley G., and Yoshihara, H.: The Flow Over a Wedge Profile at Mach Number 1. Jour. Aero. Sci., vol. 17, no. 11, Nov. 1950, pp. 723-735.
12. Kaplan, Carl: On Similarity Rules for Transonic Flows. NACA Rep. 894, 1948. (Formerly NACA TN 1527)

13. Abbott, Ira H., von Döenhoff, Albert E., and Stivers, Louis S., Jr.:
Summary of Airfoil Data. NACA Rep. 824, 1945.
14. DeYoung, John, and Harper, Charles W.: Theoretical Symmetrical
Span Loading at Subsonic Speeds for Wings Having Arbitrary Plan
Form. NACA Rep. 921, 1948.

TABLE I.- VALUES OF THE GEOMETRIC PARAMETER
 $A(t/c)^{1/3}$ FOR THE WING MODELS TESTED

A	t/c	$A(t/c)^{1/3}$	A	t/c	$A(t/c)^{1/3}$
6	0.10	2.784	2	0.04	0.684
6	.08	2.586	2	.02	.542
6	.06	2.352	1.5	.04	.513
4	.10	1.856	1.5	.02	.407
4	.08	1.724	1	.10	.464
4	.06	1.568	1	.08	.431
4	.04	1.368	1	.06	.392
3	.04	1.026	1	.04	.342
2	.10	.928	1	.02	.271
2	.08	.862	.5	.04	.171
2	.06	.784	.5	.02	.136



TABLE II.- NUMERICAL VALUES OF $(t/c)^{1/3}$,
 $(t/c)^{2/3}$, AND $(t/c)^{5/3}$

t/c	$(t/c)^{1/3}$	$(t/c)^{2/3}$	$(t/c)^{5/3}$
0.12	0.493	0.243	0.0293
.11	.479	.230	.0254
.10	.464	.216	.0217
.09	.448	.201	.0181
.08	.431	.186	.0148
.07	.412	.170	.0118
.06	.392	.154	.0092
.05	.368	.136	.0068
.04	.342	.117	.00468
.03	.311	.097	.00292
.02	.271	.073	.00147

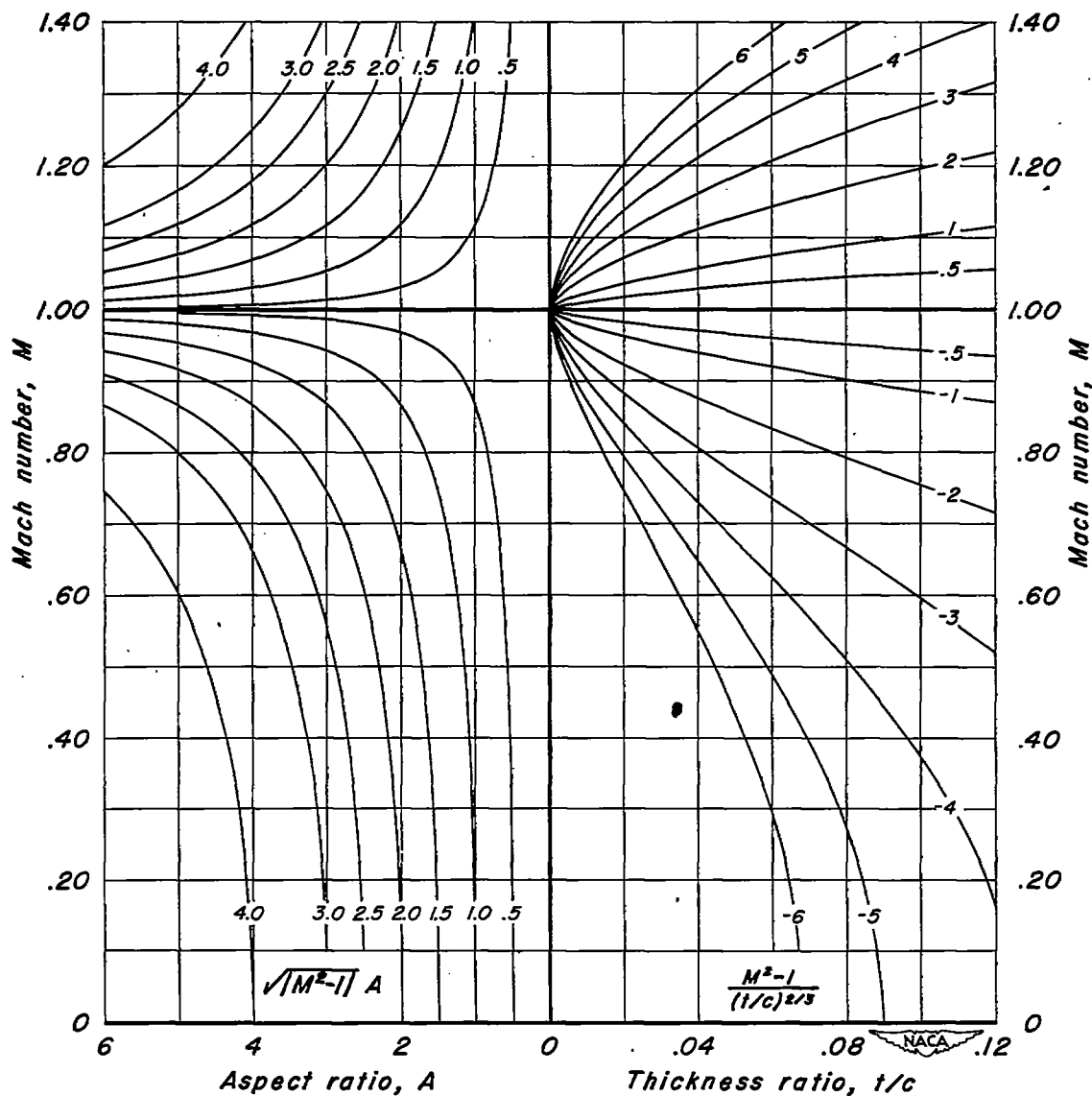


NACA

TABLE III.- VALUES OF THE ANGLE OF ATTACK (IN DEGREES)
FOR VARIOUS VALUES OF THE RATIO $\frac{\alpha}{t/c}$ (IN RADIANS)

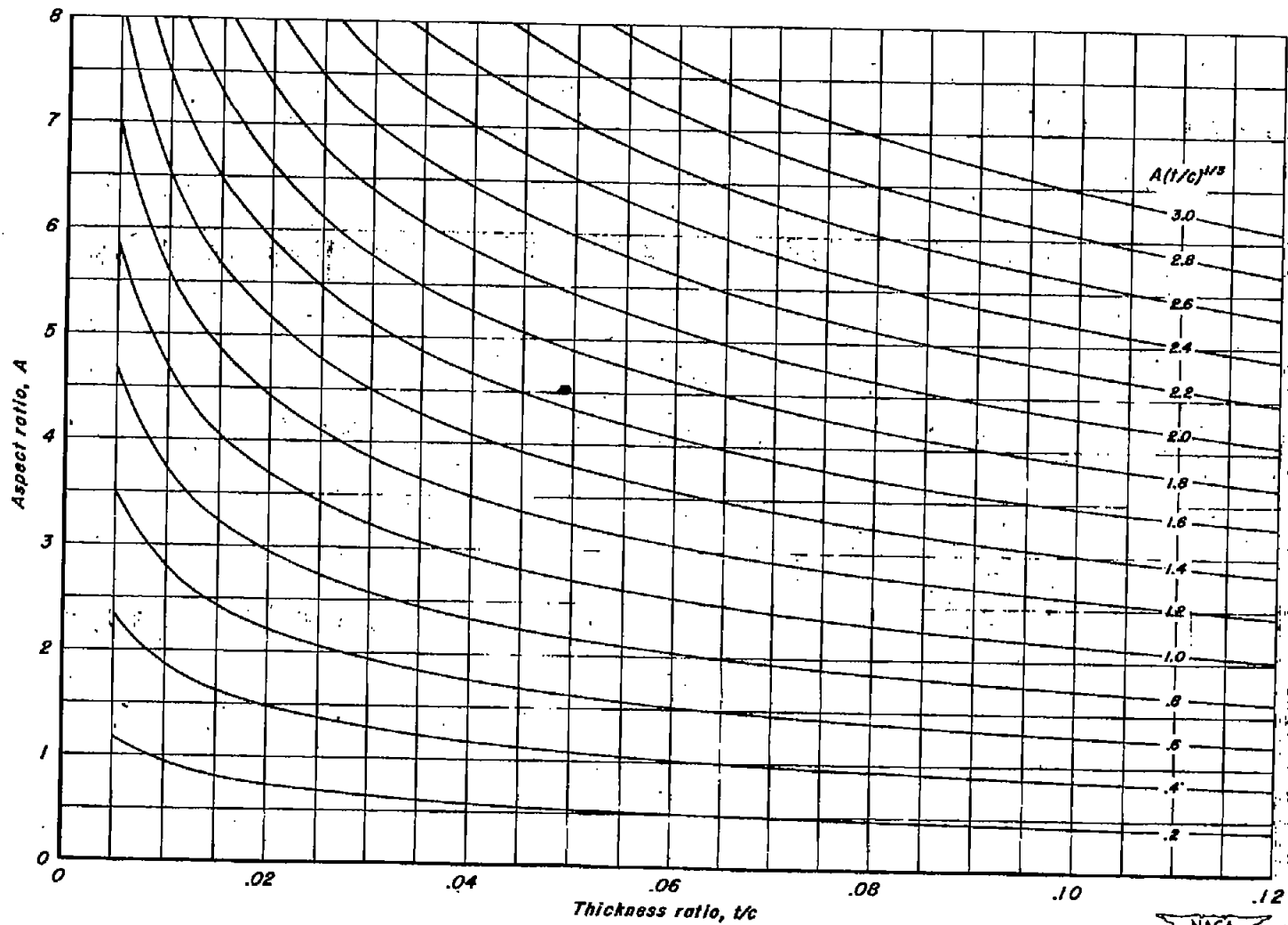
t/c	Angle of attack α , degrees			
	$\frac{\alpha}{t/c}$, 0.5 radian	1.0 radian	1.5 radians	2.0 radians
0.10	2.87	5.73	8.60	--
.08	2.29	4.58	6.87	--
.06	1.72	3.44	5.16	6.87
.04	--	2.29	3.44	4.58
.02	--	--	1.72	2.29





(a) The functional variation of aspect ratio and thickness ratio with Mach number.

Figure 1.- Requirements for similitude of transonic flow.



(b) The functional variation between thickness ratio and aspect ratio.
Figure 1.— Concluded.

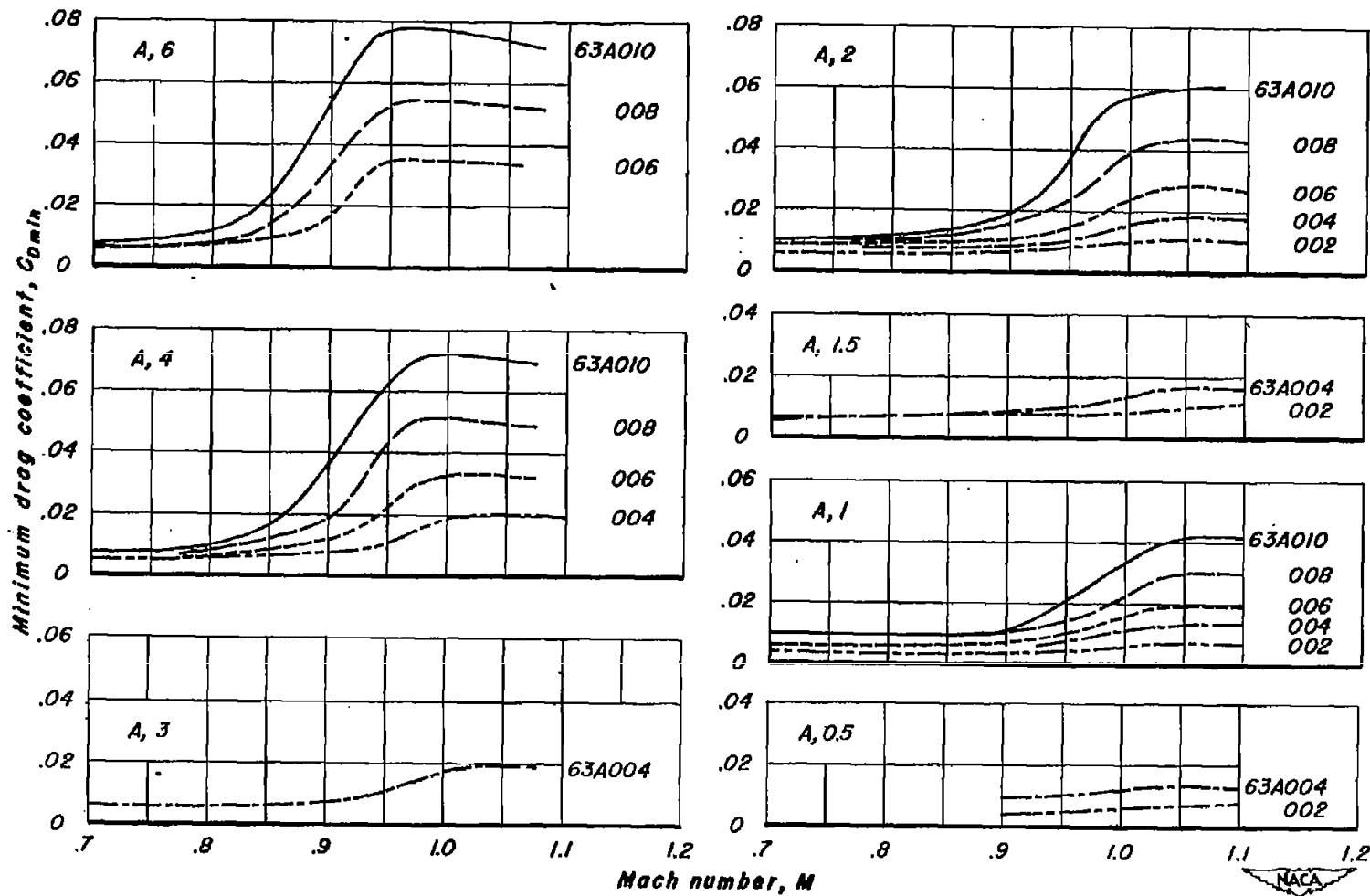


Figure 2.- The variation of minimum drag coefficient with Mach number.

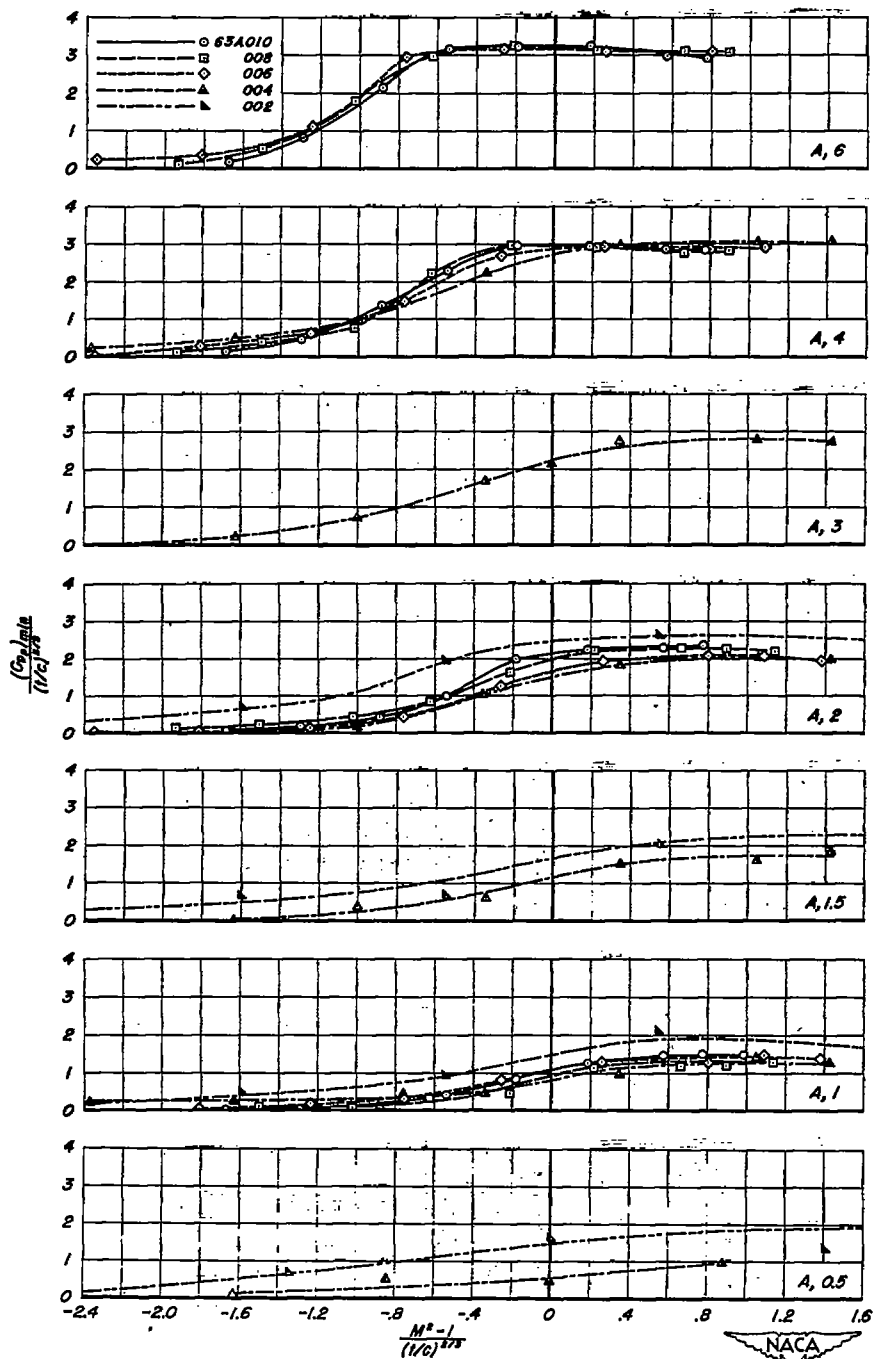


Figure 3.- The variation of $\frac{(C_D)_{min}}{(1/c)^{2/3}}$ with $\frac{M^2 - 1}{(1/c)^{2/3}}$ for the various aspect ratios and thickness ratios.

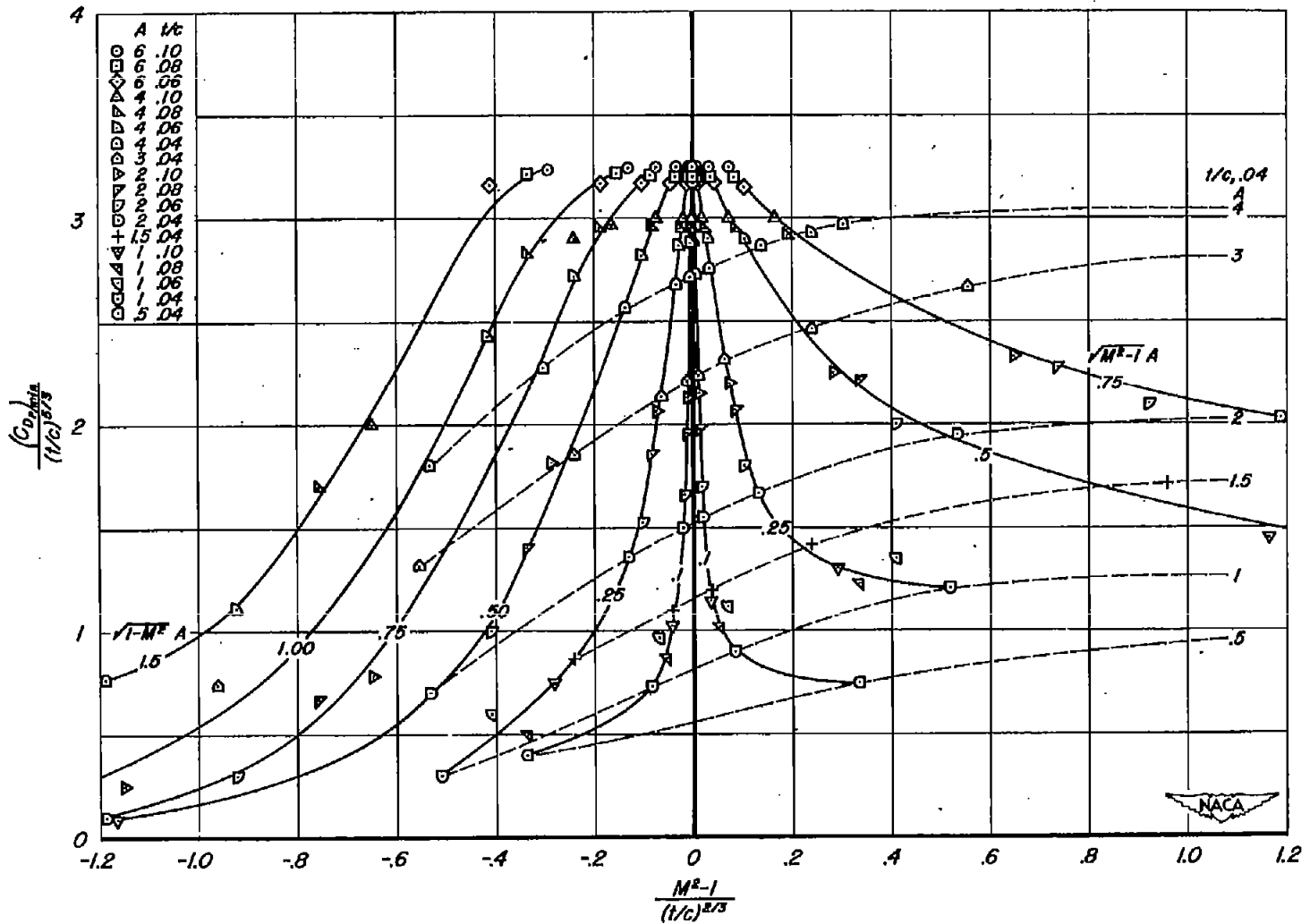


Figure 4.- The correlation of the generalized minimum pressure drag coefficient for constant values of $\sqrt{M^2-1} A$.

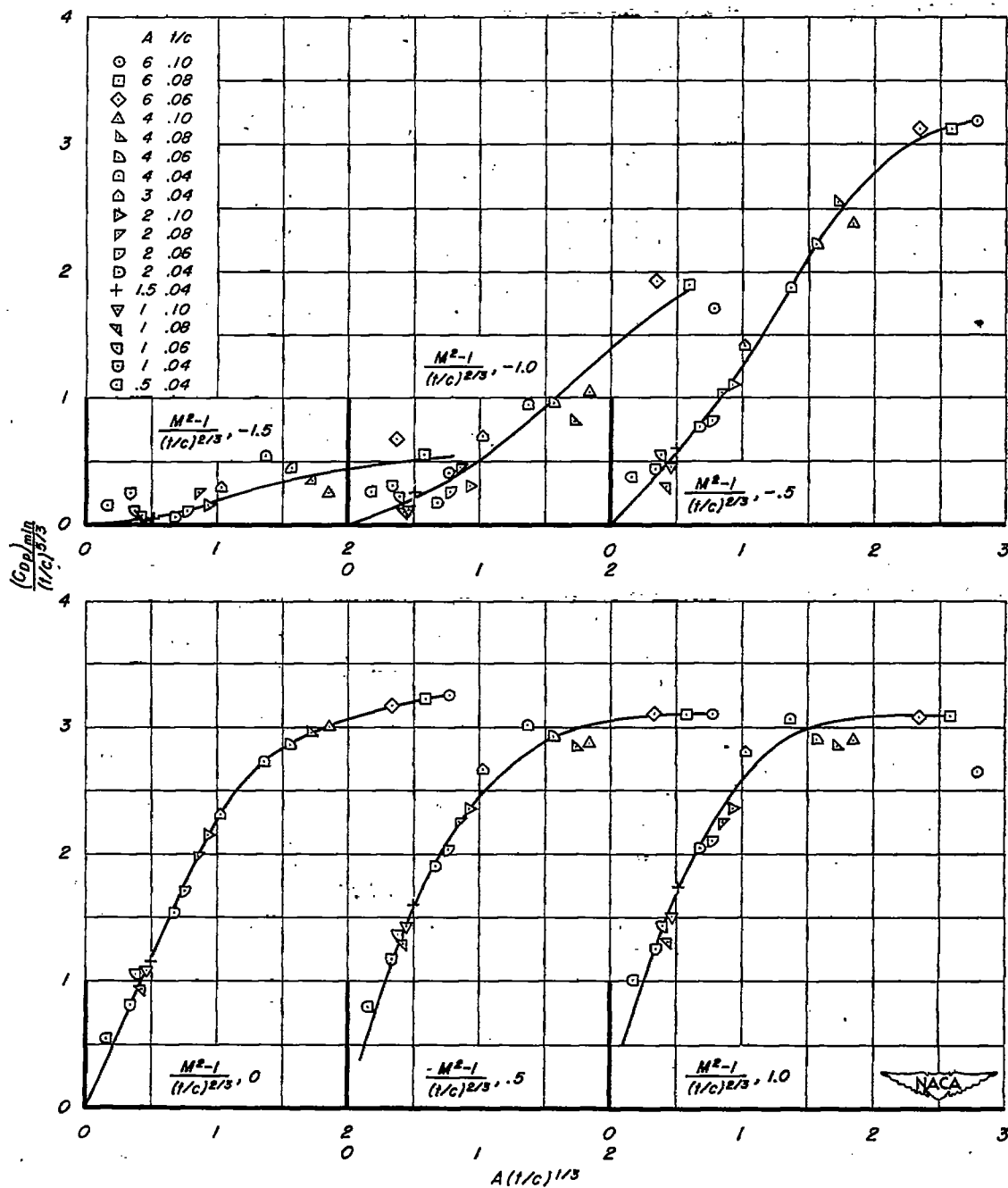


Figure 5.- The correlation of the generalized minimum pressure-drag coefficient for constant values of the speed parameter.

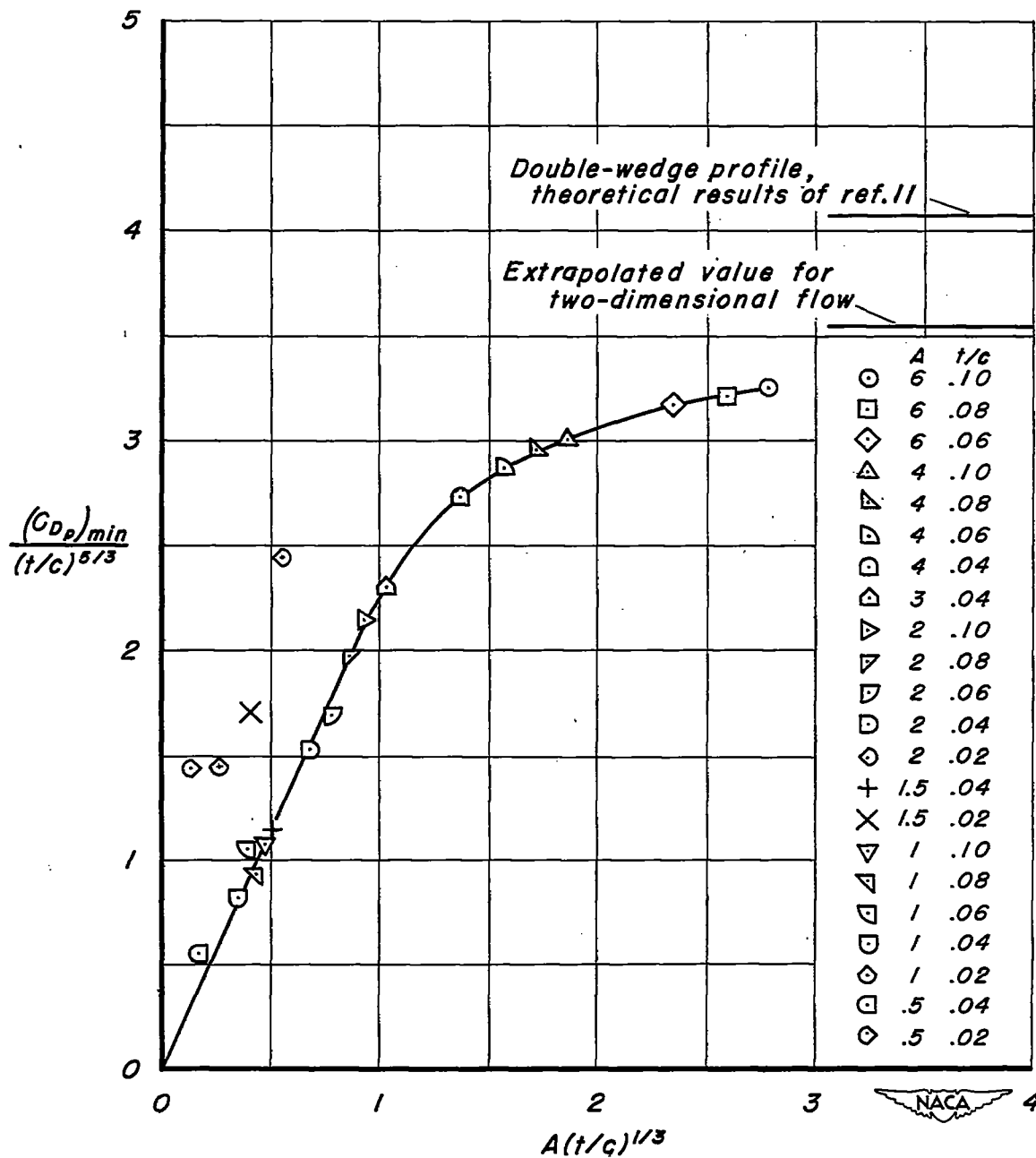


Figure 6.—Correlation of $\frac{(C_{Dp})_{min}}{(t/c)^{5/3}}$ at $M=1$.

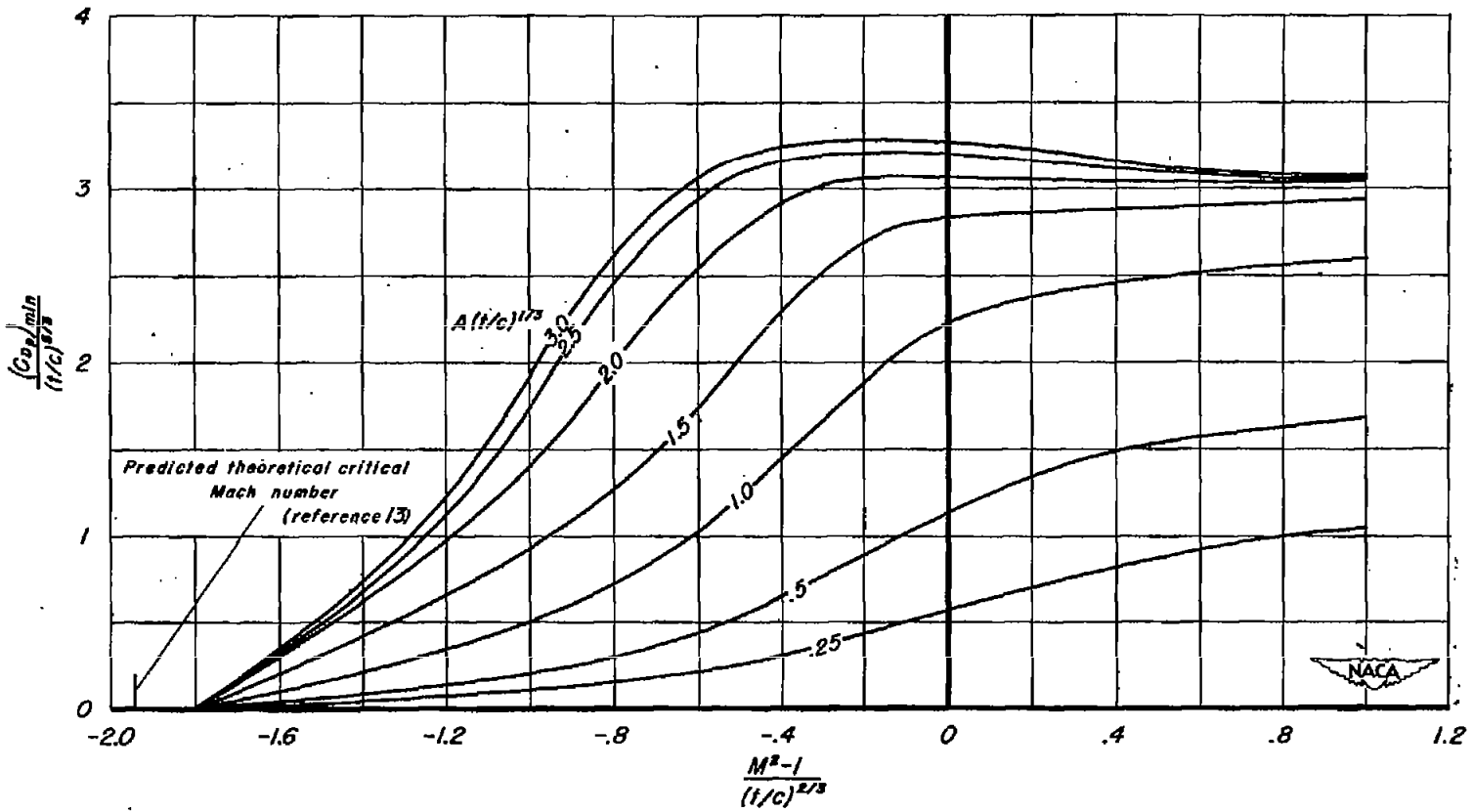


Figure 7.- Summary curves for the generalized minimum pressure-drag coefficient.

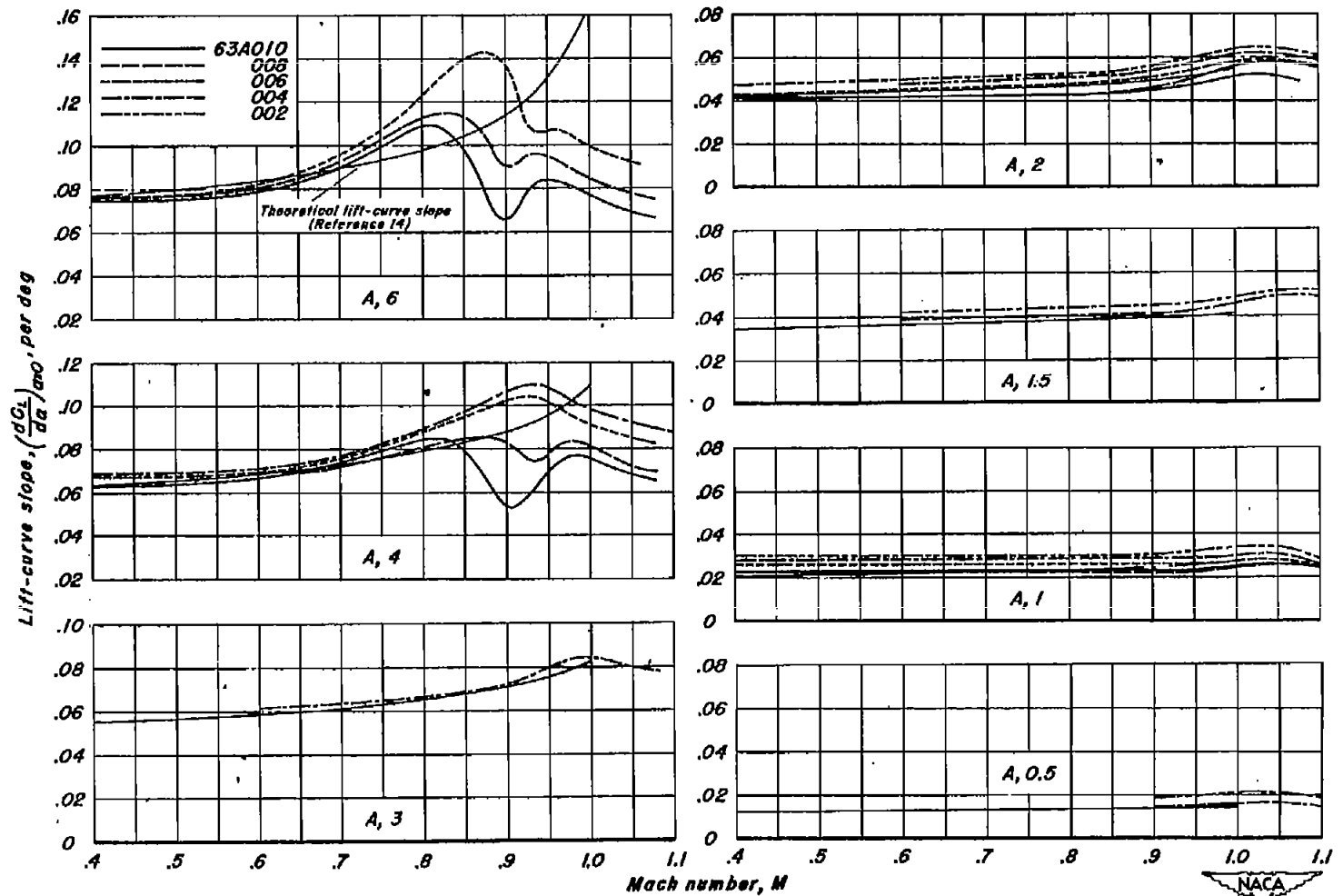


Figure 8.—The variation of lift-curve slope with Mach number.

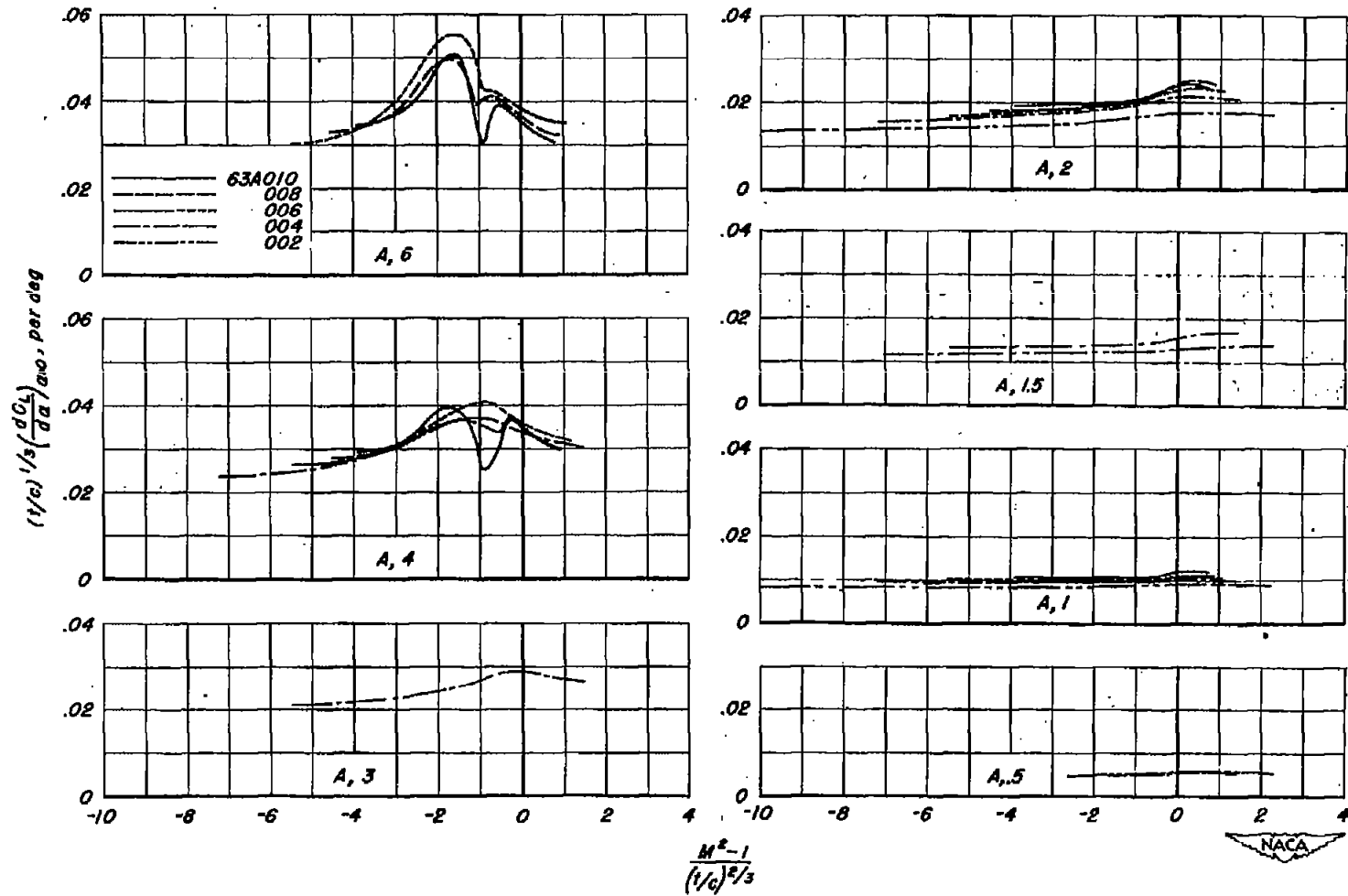
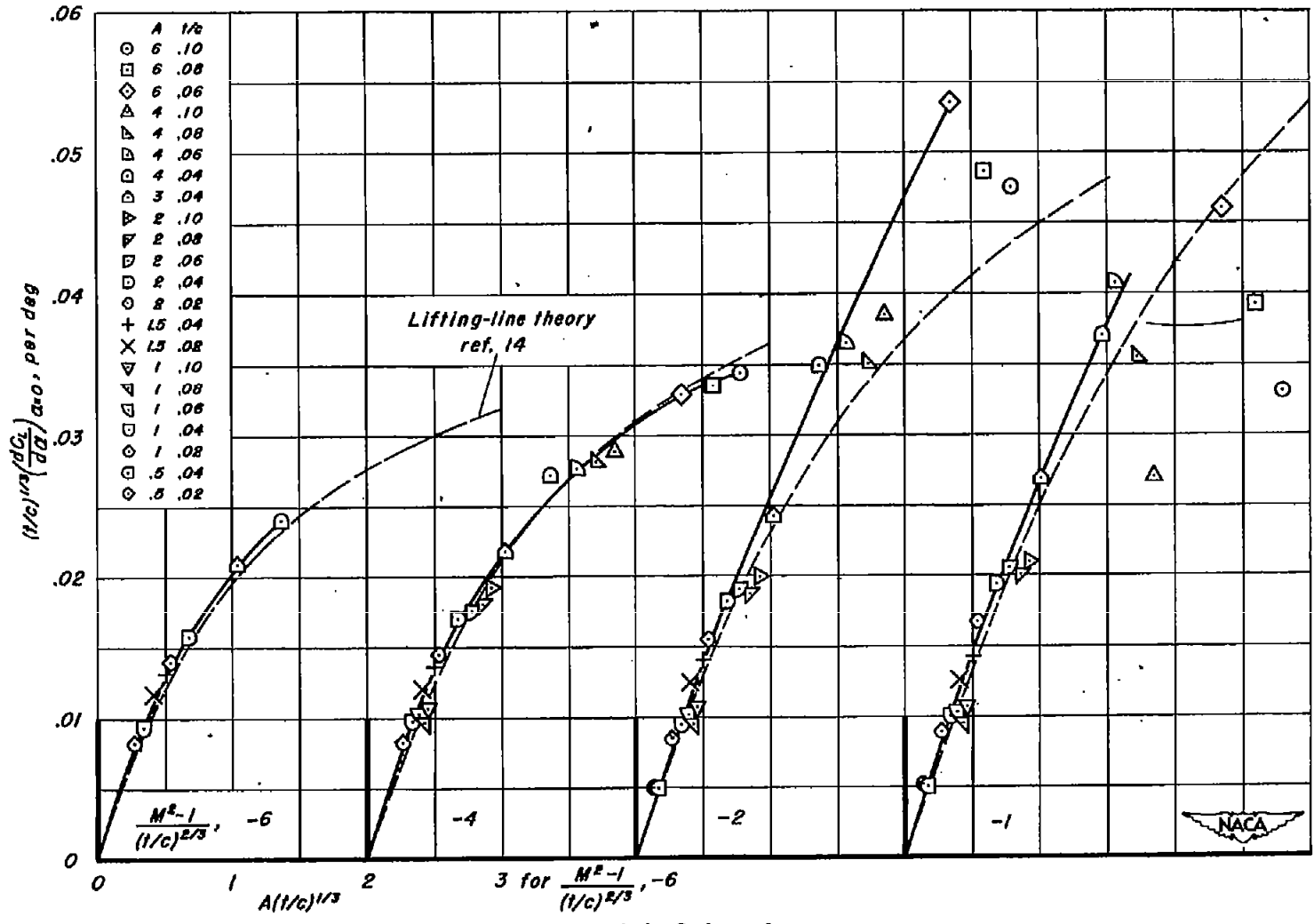
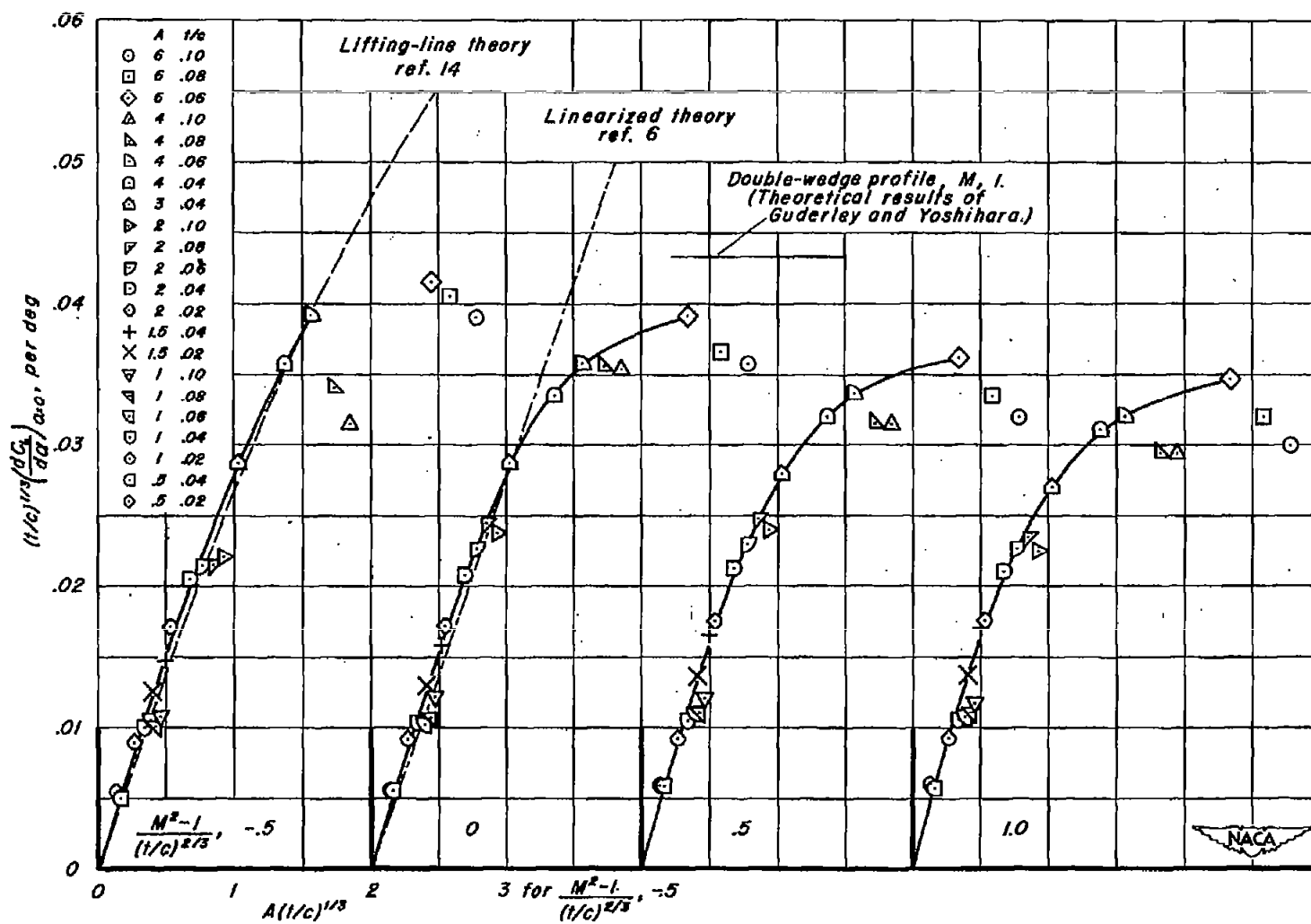


Figure 9.- The variation of the generalized lift-curve slope with the speed parameter.



CONFIDENTIAL

(a) Subsonic.
Figure 10.- Correlation of the generalized lift-curve slope.



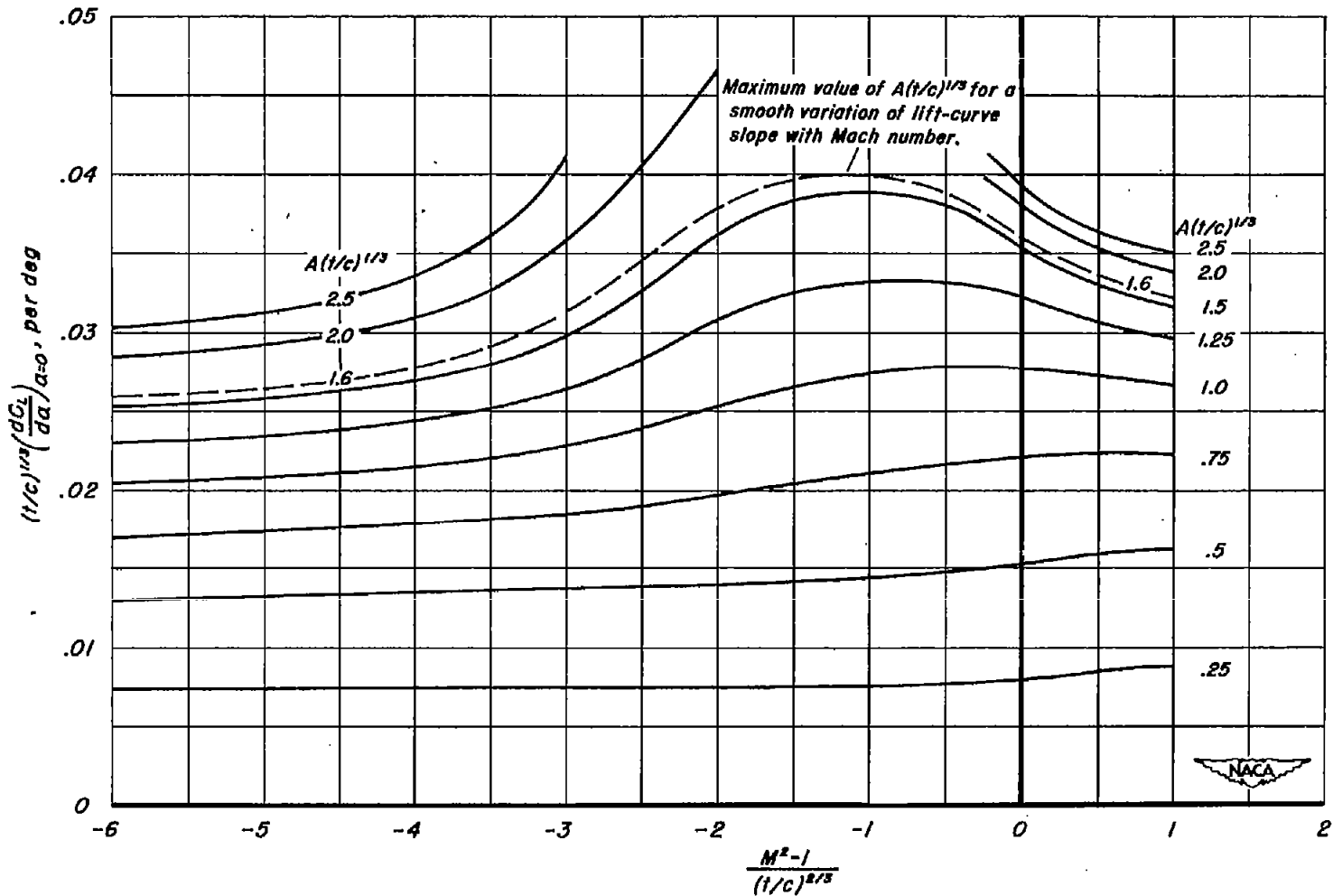


Figure 11.- Summary curves for the generalized lift-curve slope.

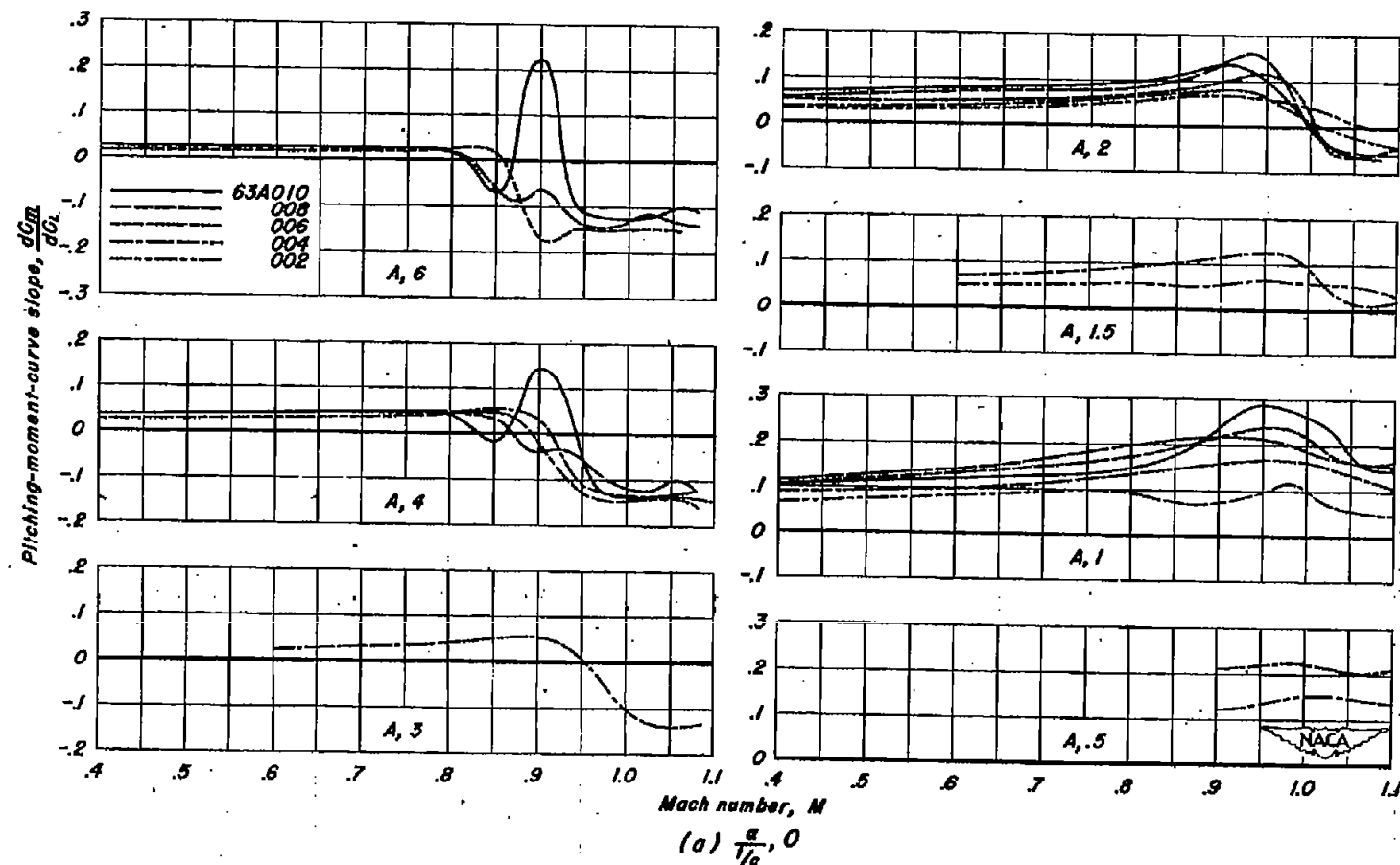
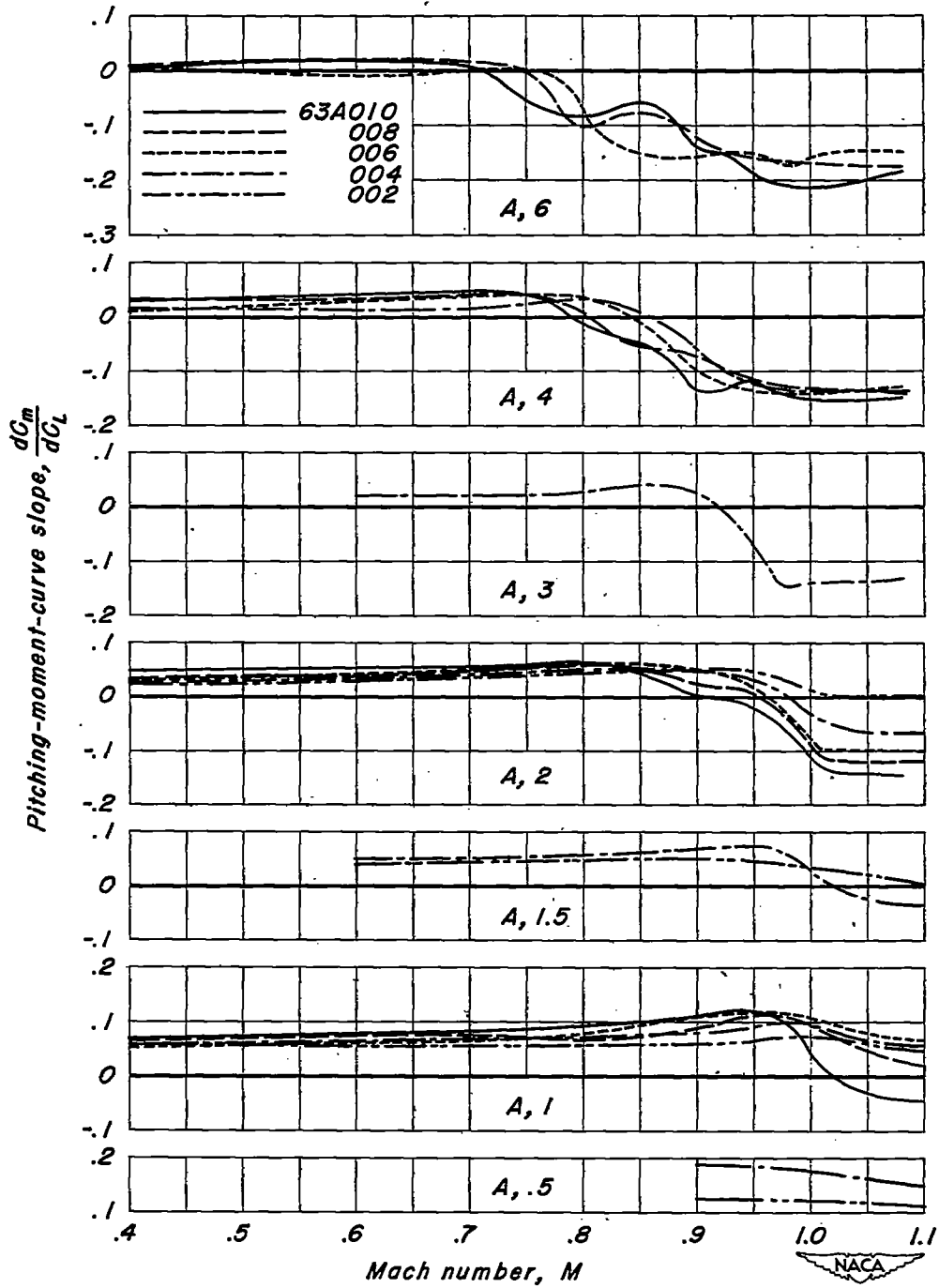


Figure 12.—The variation of pitching-moment-curve slope with Mach number.

CONFIDENTIAL

CONFIDENTIAL



(b) $\frac{a}{1/c}$

Figure 12.- Continued.

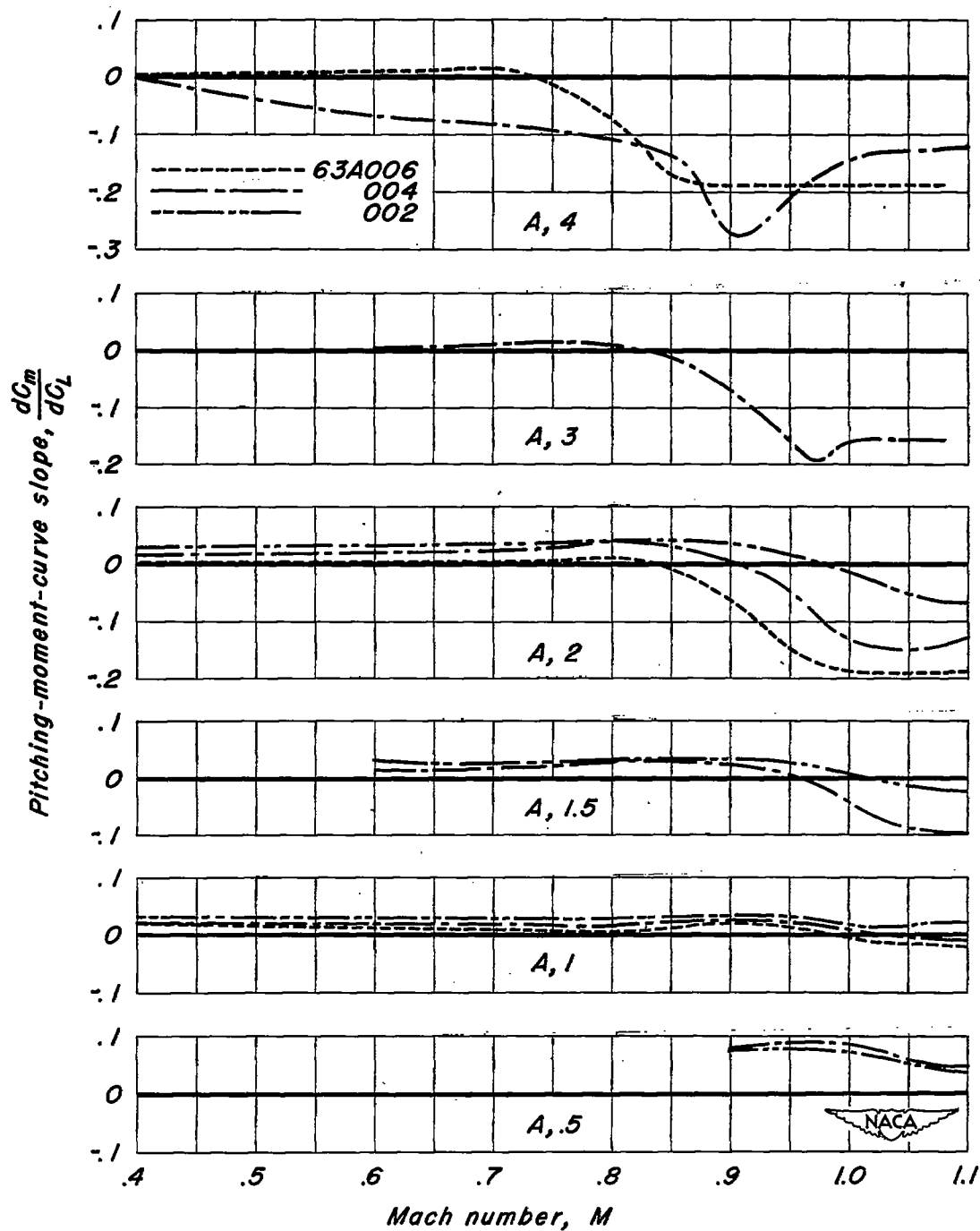
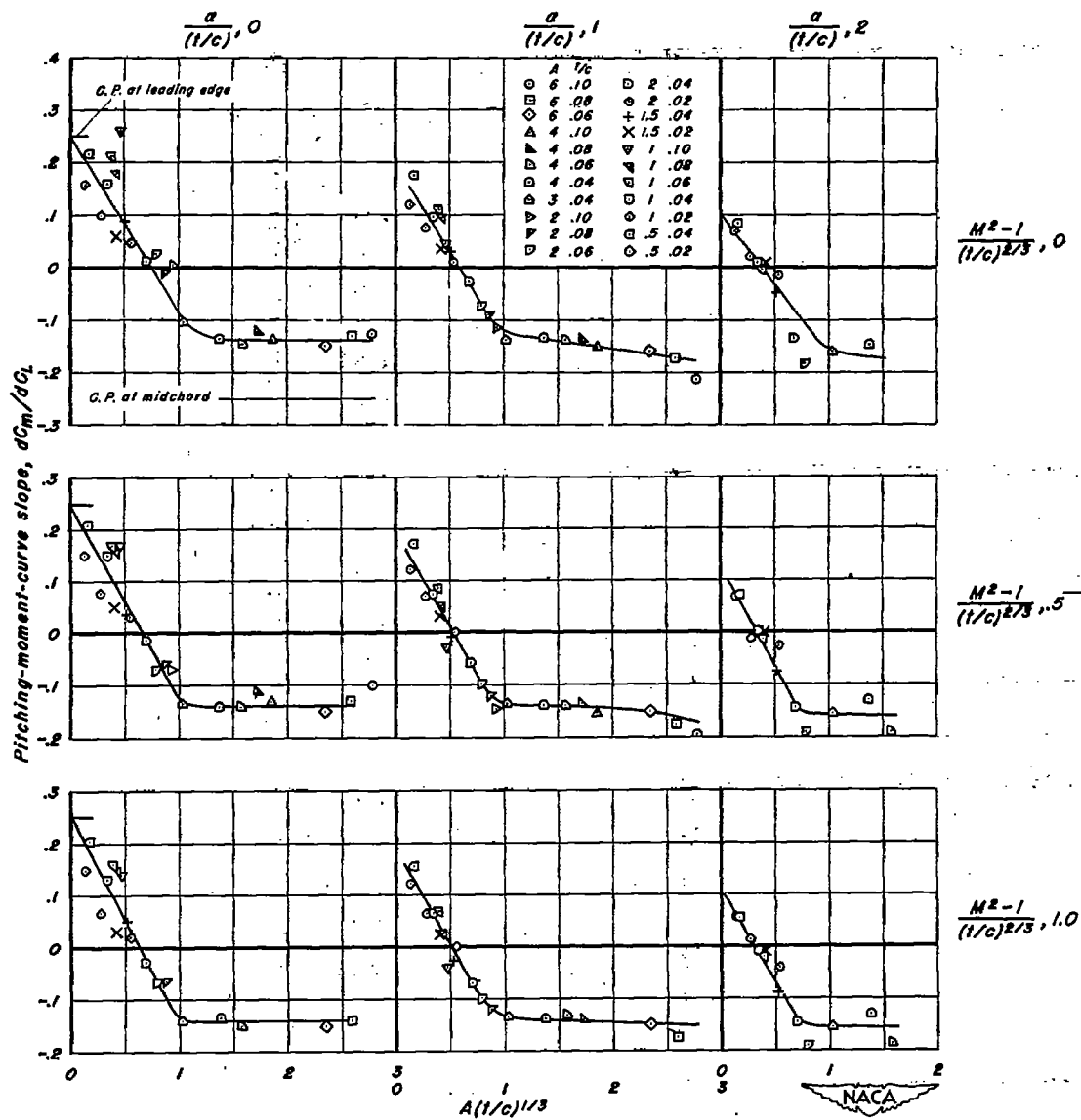
~~CONFIDENTIAL~~(c) $\frac{a}{c}$, 2.0
 $\frac{1}{c}$

Figure 12.- Concluded.

~~CONFIDENTIAL~~



(b) Sonic and supersonic.
 Figure 13.- Concluded.

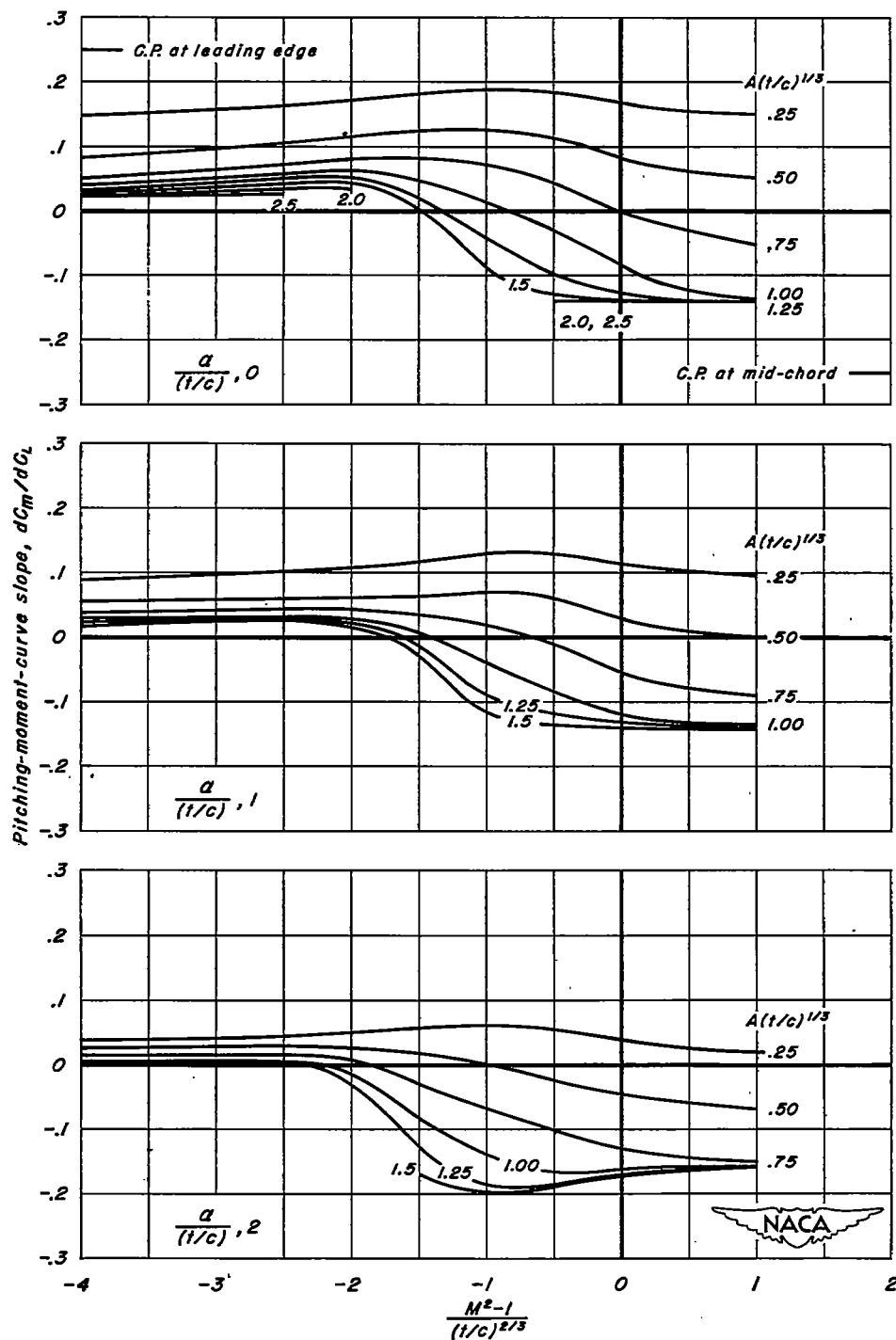
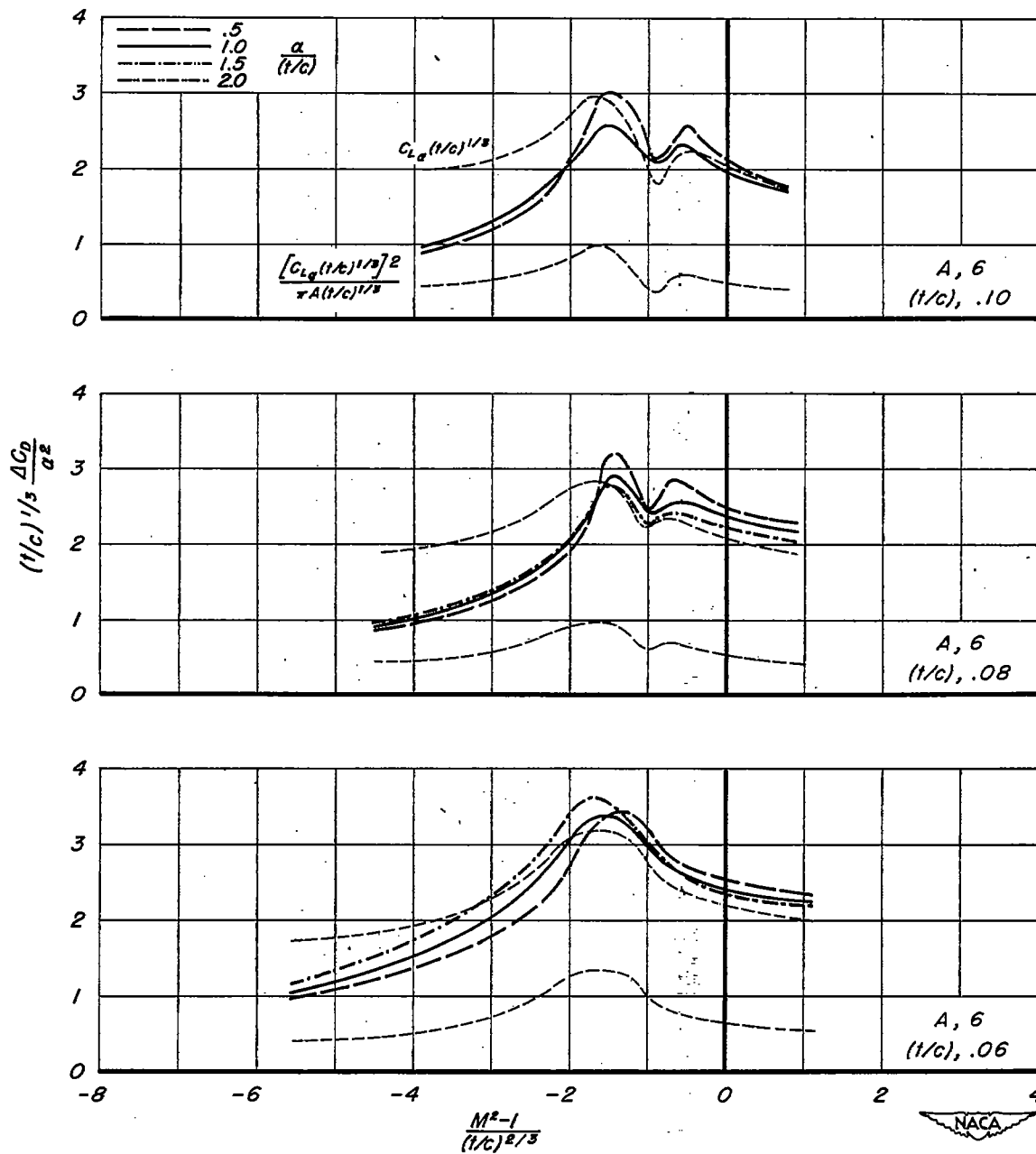
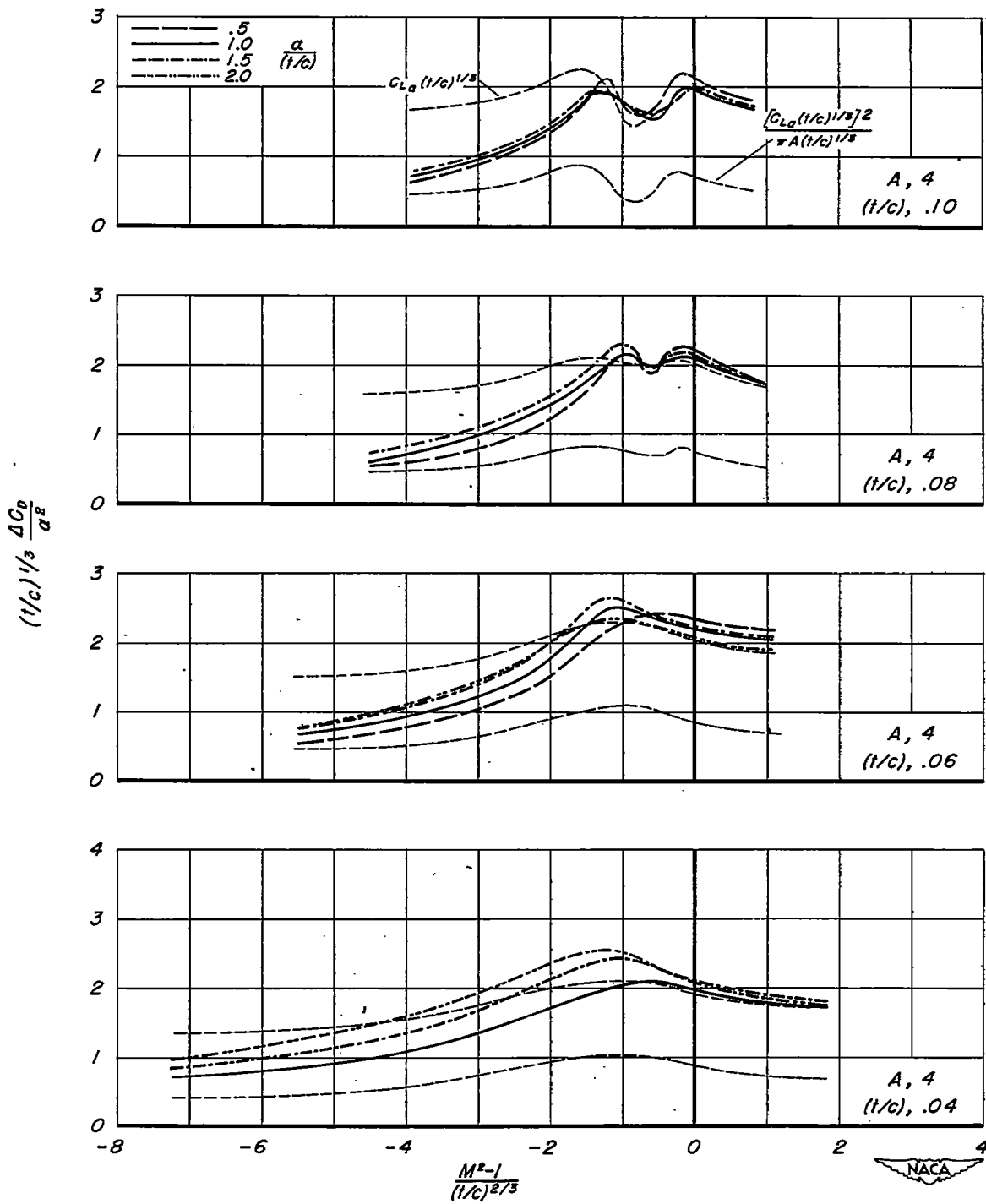


Figure 14.- Summary curves for pitching-moment-curve slope.

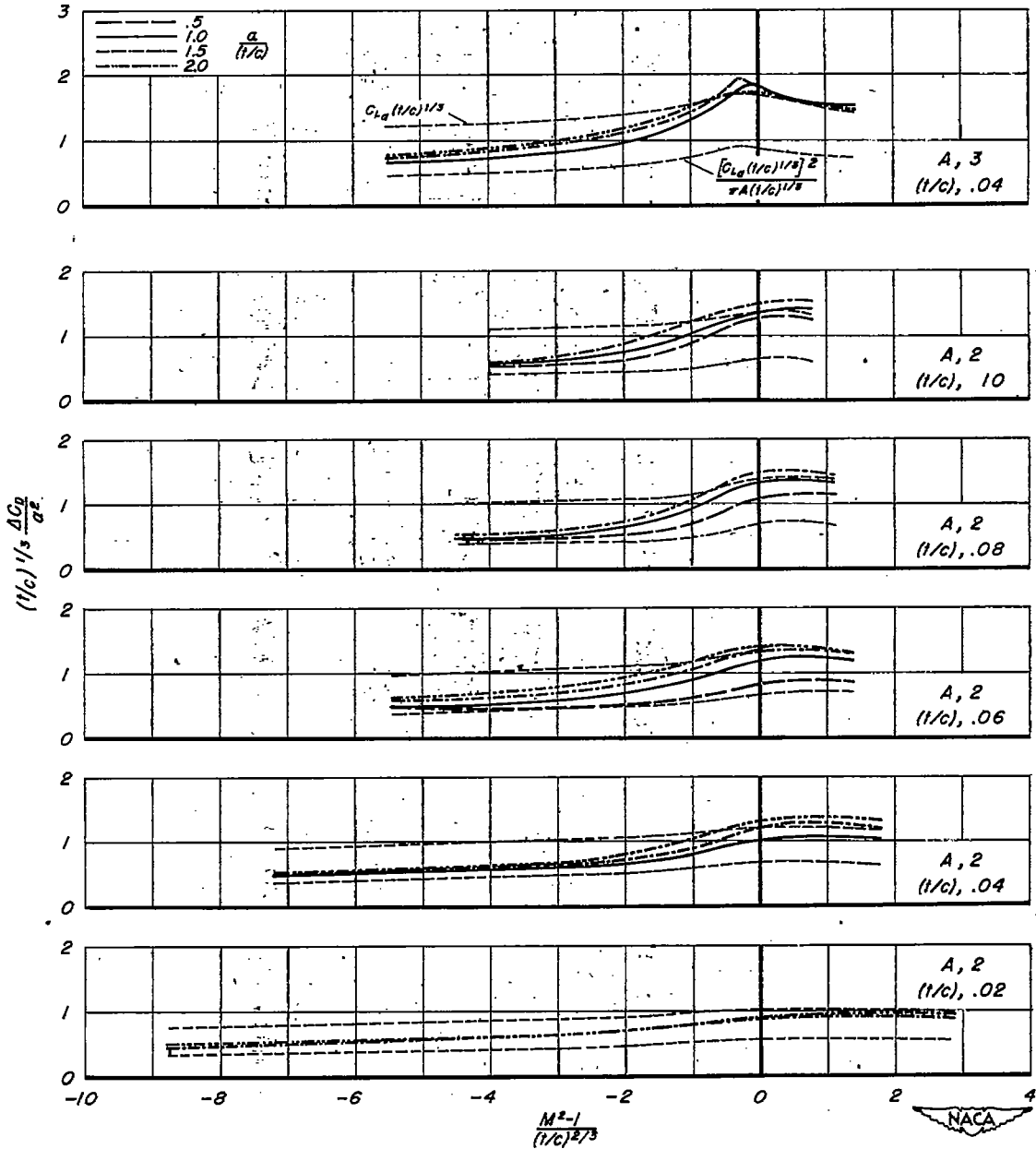


(a) A, 6

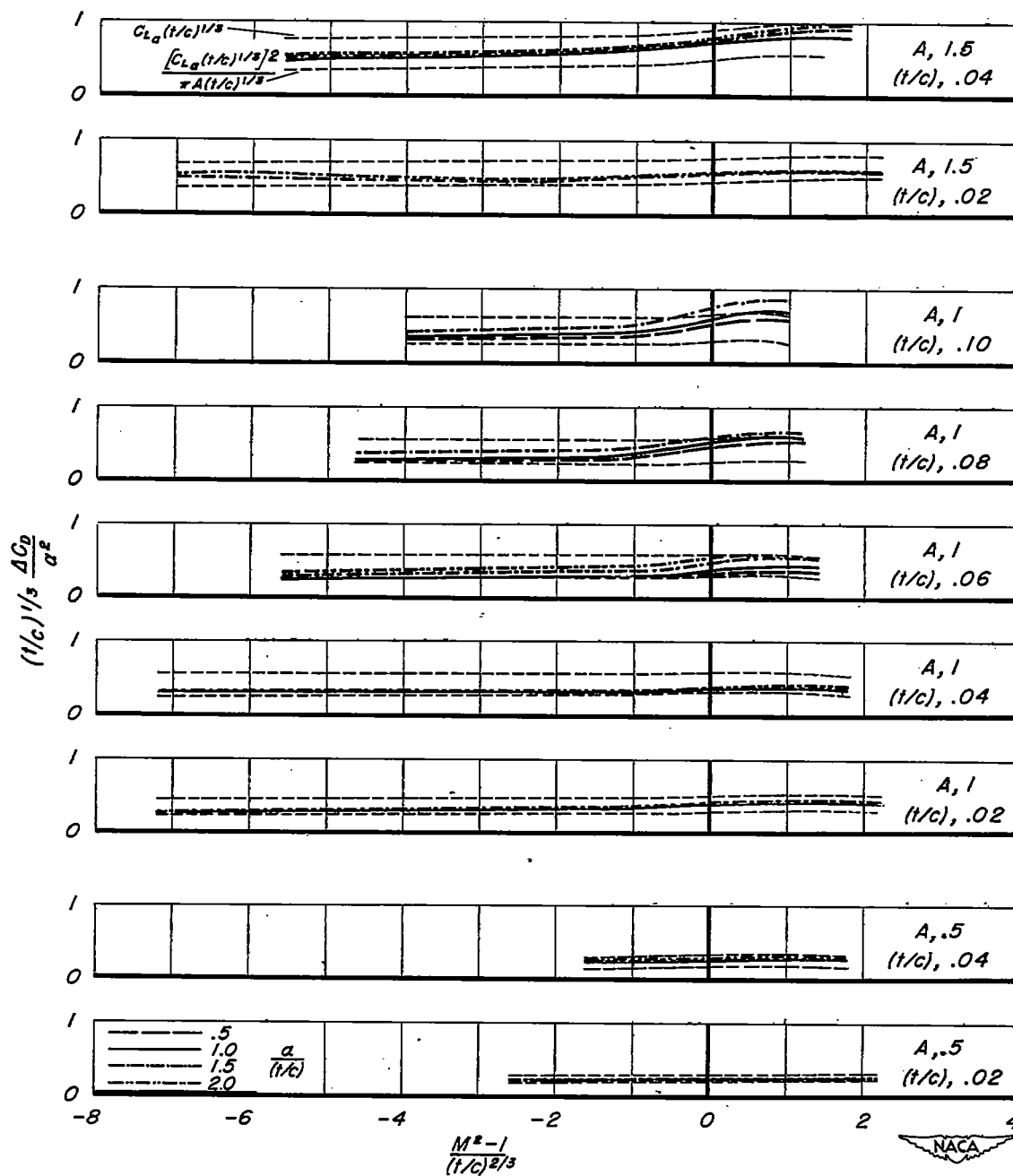
Figure 15.- The variation of the generalized drag-due-to-lift parameter $(t/c)^{1/3} \frac{\Delta C_D}{\alpha^2}$ with the speed parameter $\frac{M^2-1}{(t/c)^{2/3}}$ for several ratios of $a/(t/c)$. a in radians.



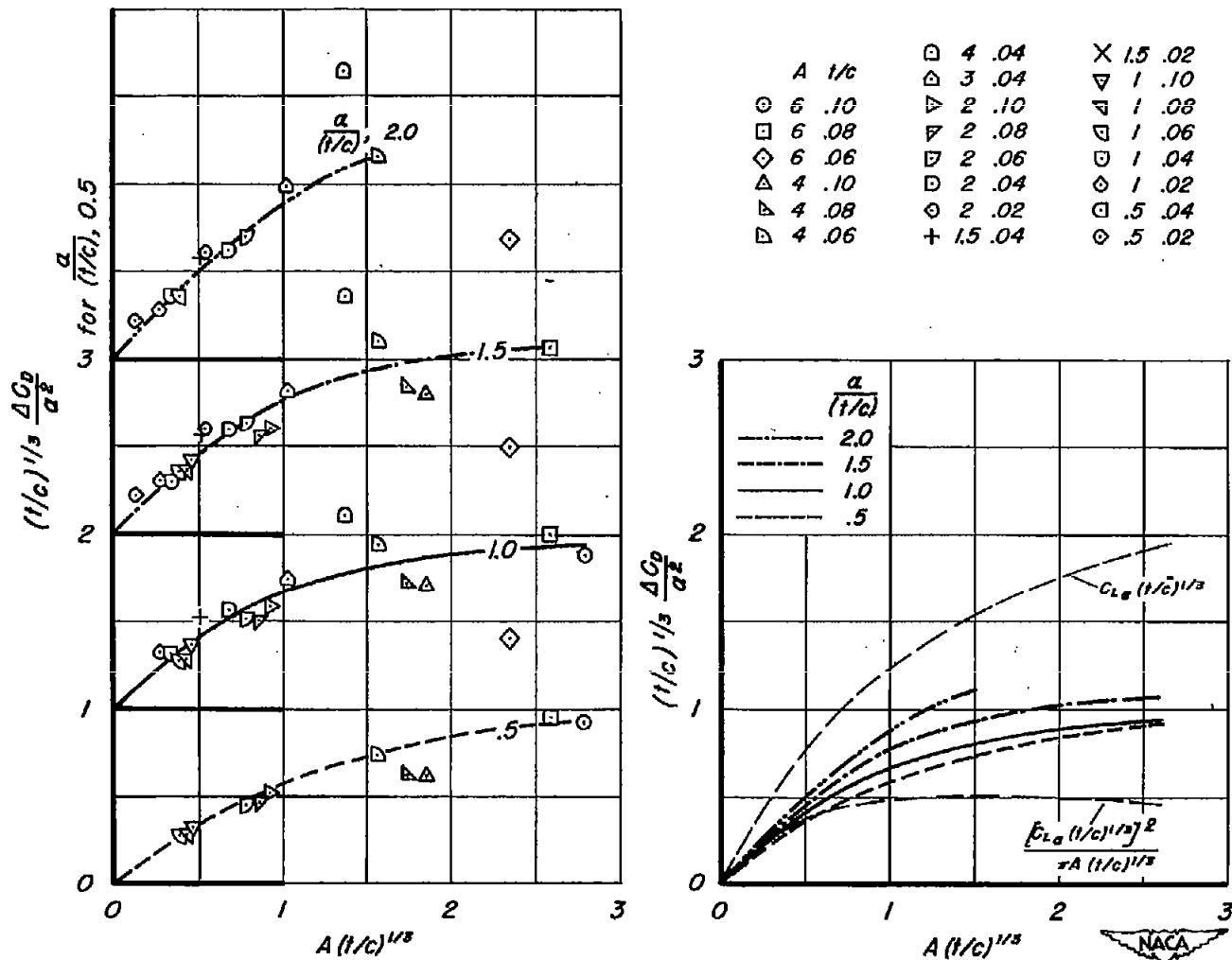
(b) A, 4
Figure 15.- Continued.



(c) A, 3 and 2
Figure 15.- Continued.

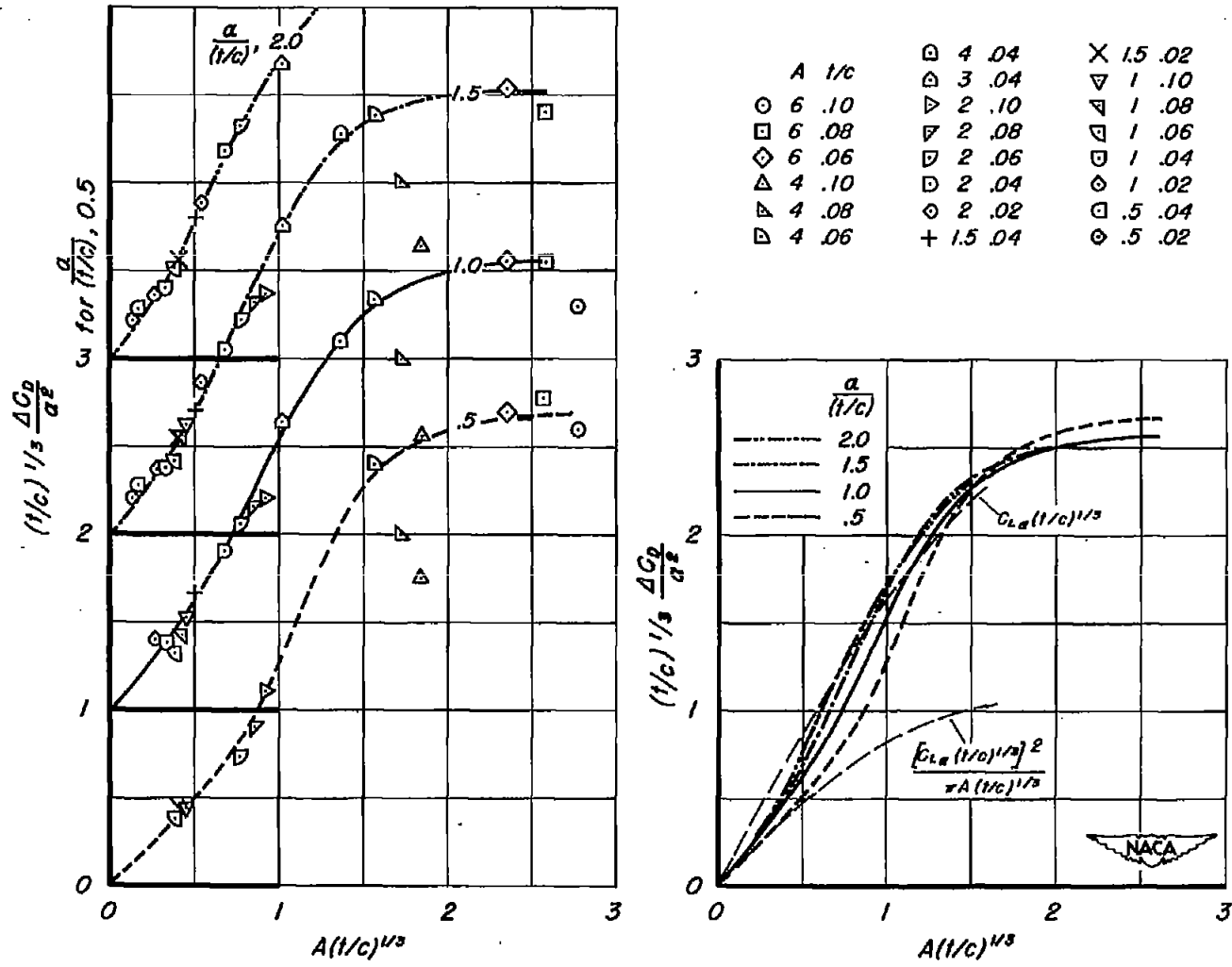


(d) $A, 1.5, 1, \text{ and } .5$
Figure 15.- Concluded.



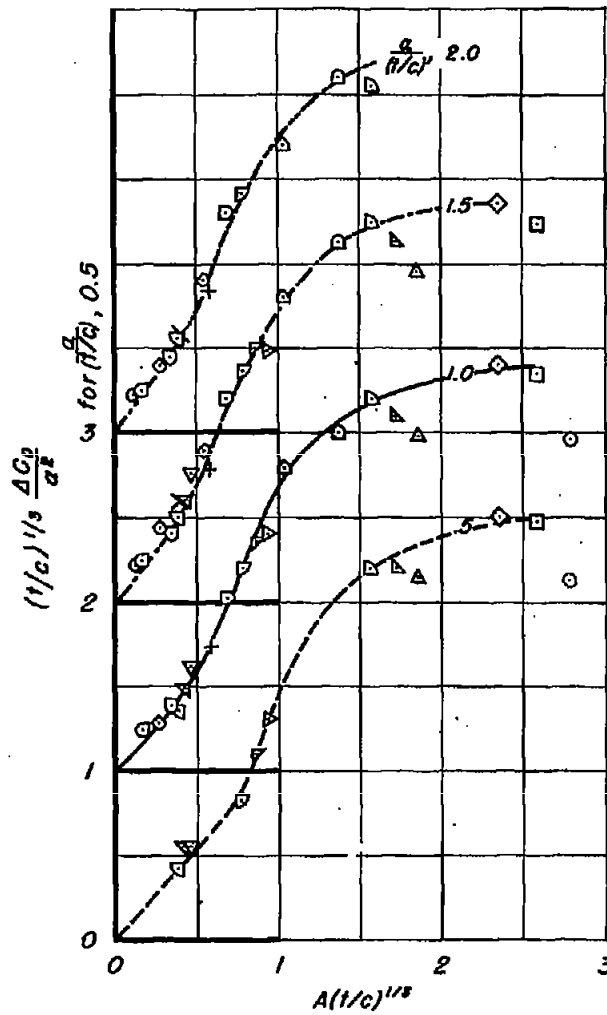
$$(a) \frac{M^2 - 1}{(t/c)^{2/3}} - 4$$

Figure 16.- Correlation of $(t/c)^{1/3} \frac{\Delta C_D}{\sigma^2}$ for several values of the speed parameter.

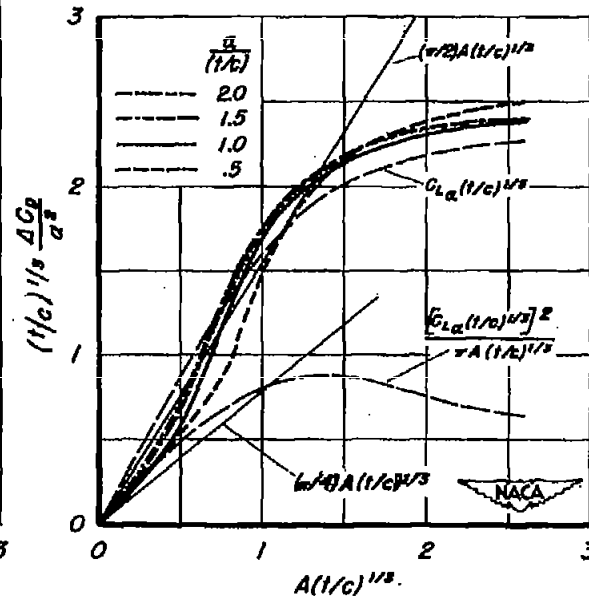


(b) $\frac{M^2-1}{(1/c)^{2/3}}, .5$

Figure 16.- Continued.

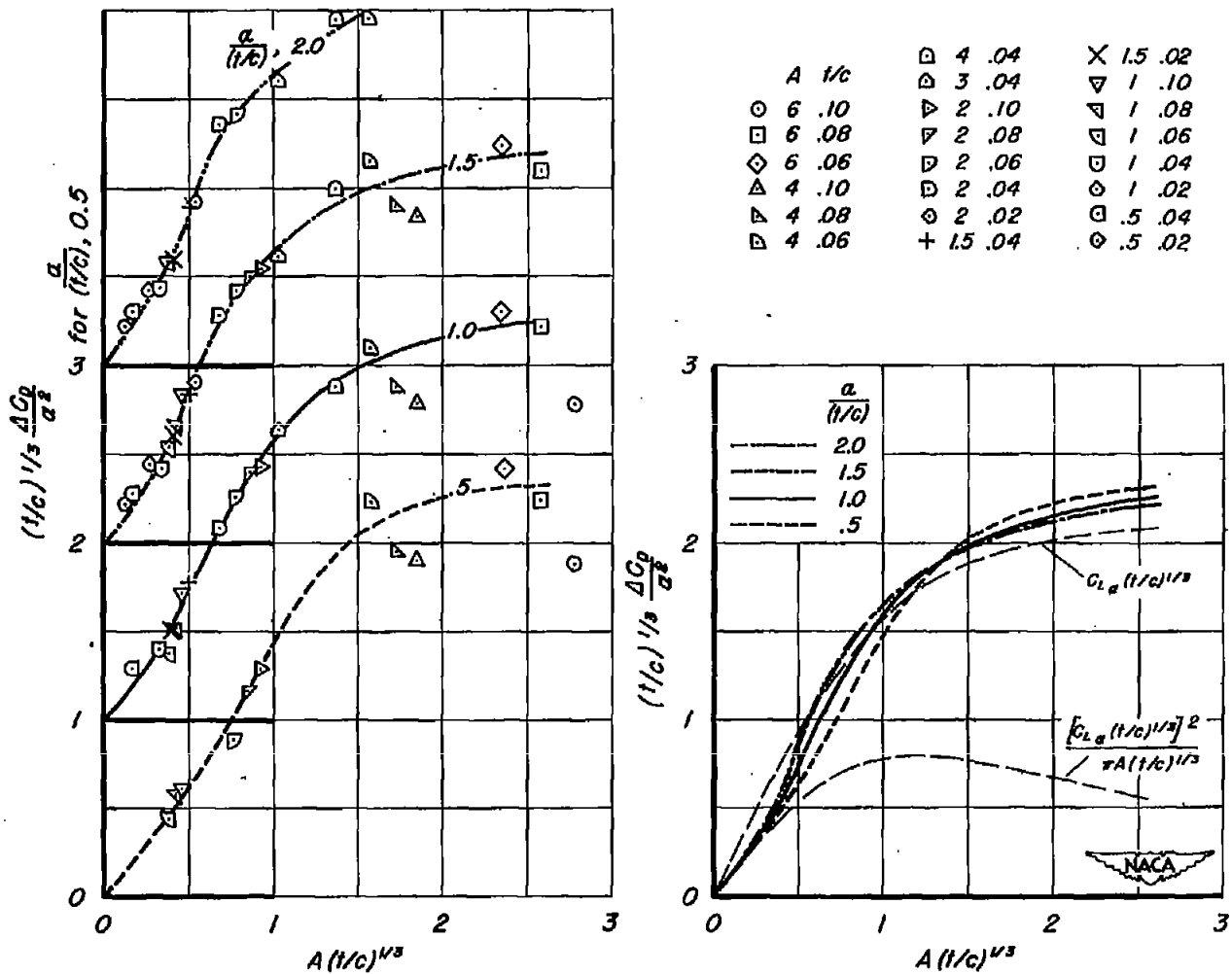


\circ	6 .10	\square	4 .04	\times	1.5 .02
\square	6 .08	∇	3 .04	∇	1 .10
\diamond	6 .06	∇	2 .10	∇	1 .08
\triangle	4 .10	∇	2 .08	∇	1 .06
∇	4 .08	∇	2 .06	\square	1 .04
∇	4 .06	\diamond	2 .04	\circ	1 .02
		\diamond	2 .02	\square	.5 .04
		$+$	1.5 .04	\diamond	.5 .02



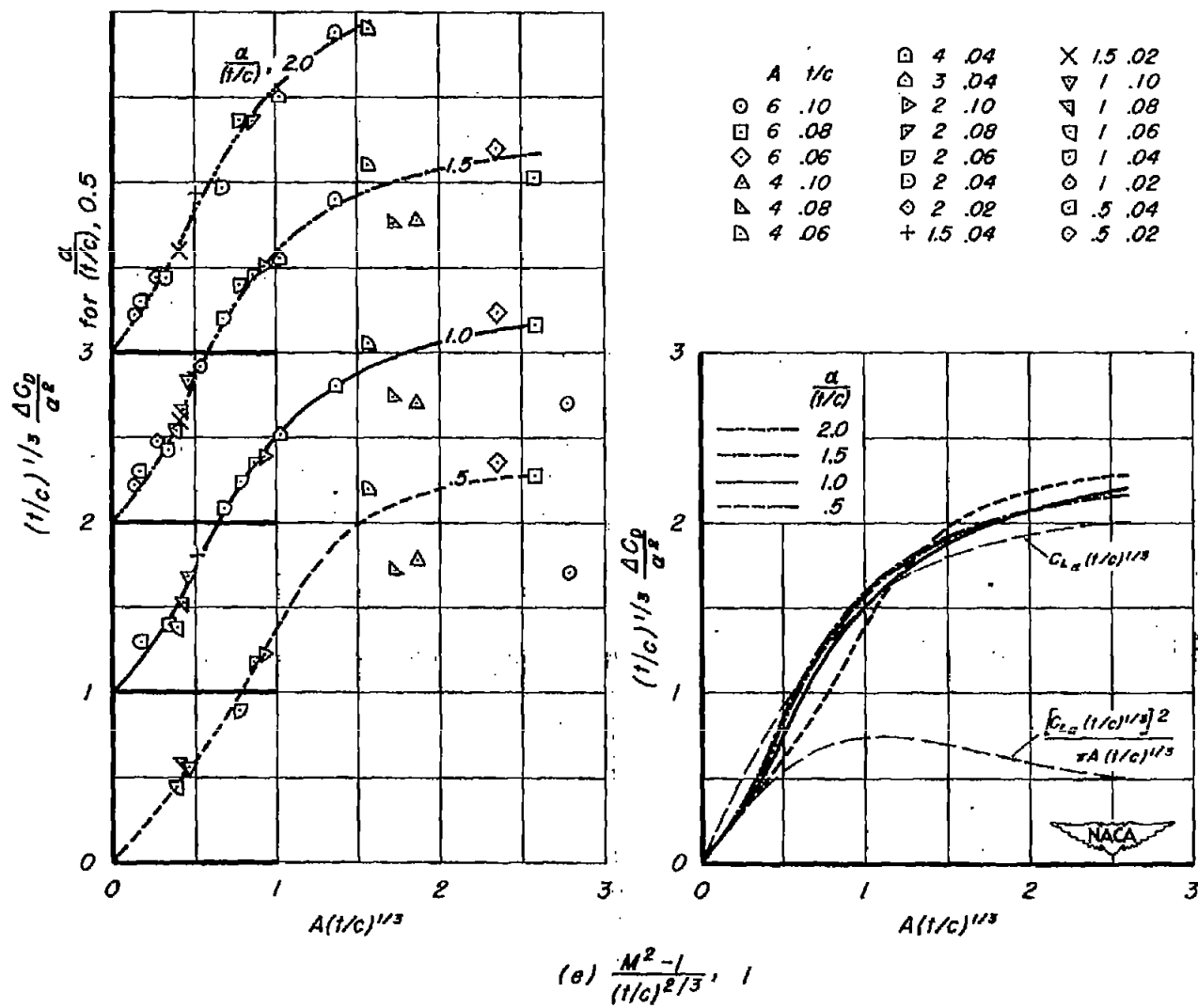
$$(c) \frac{M^2 - 1}{(t/c)^{2/3}} = 0$$

Figure 16.- Continued.



(d) $\frac{M^2-1}{(1/c)^{2/3}} = 0.5$

Figure 16.- Continued.



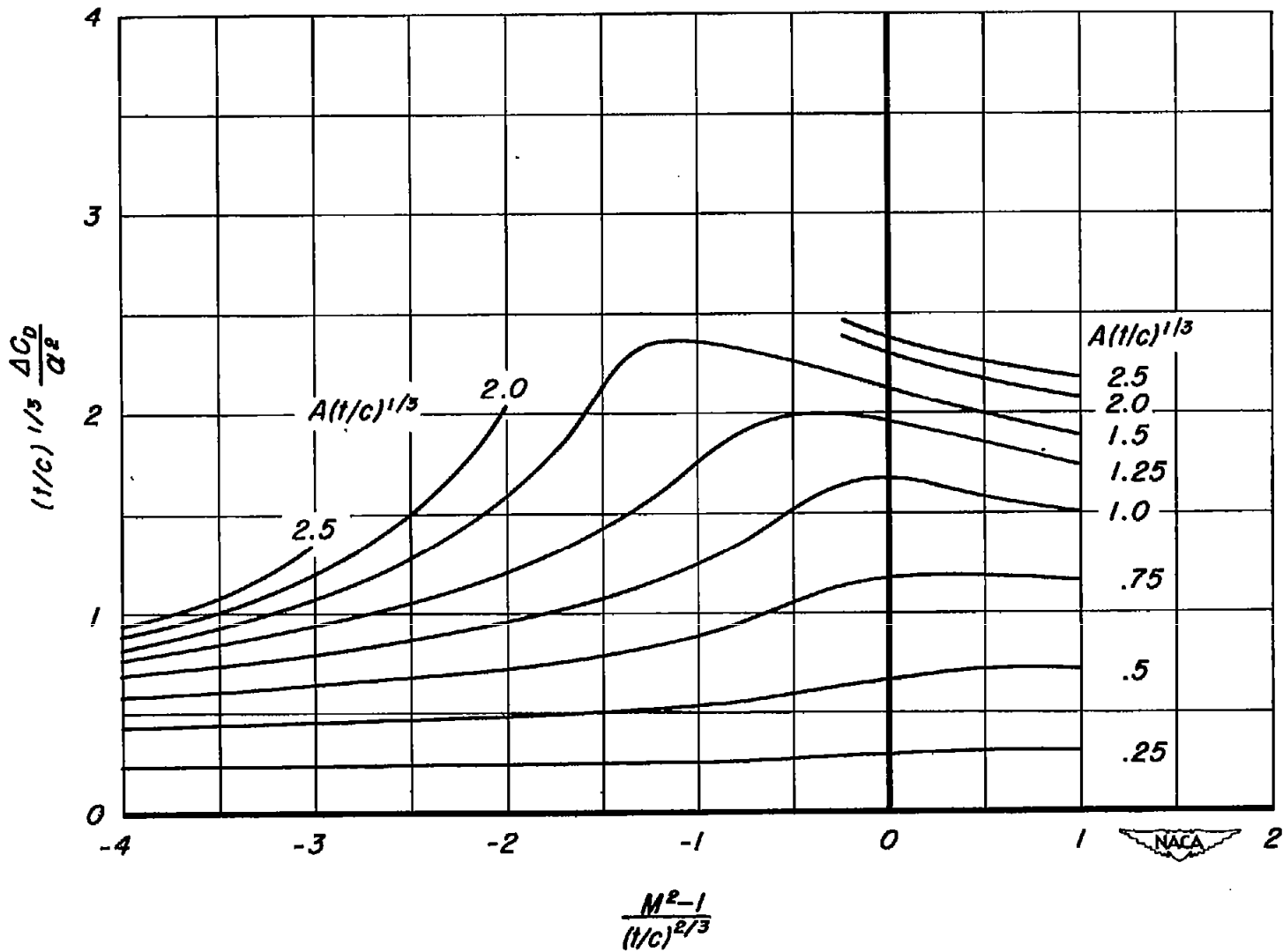


Figure 17.- Summary curves for $(t/c)^{1/3} \frac{\Delta C_D}{a^2}$.

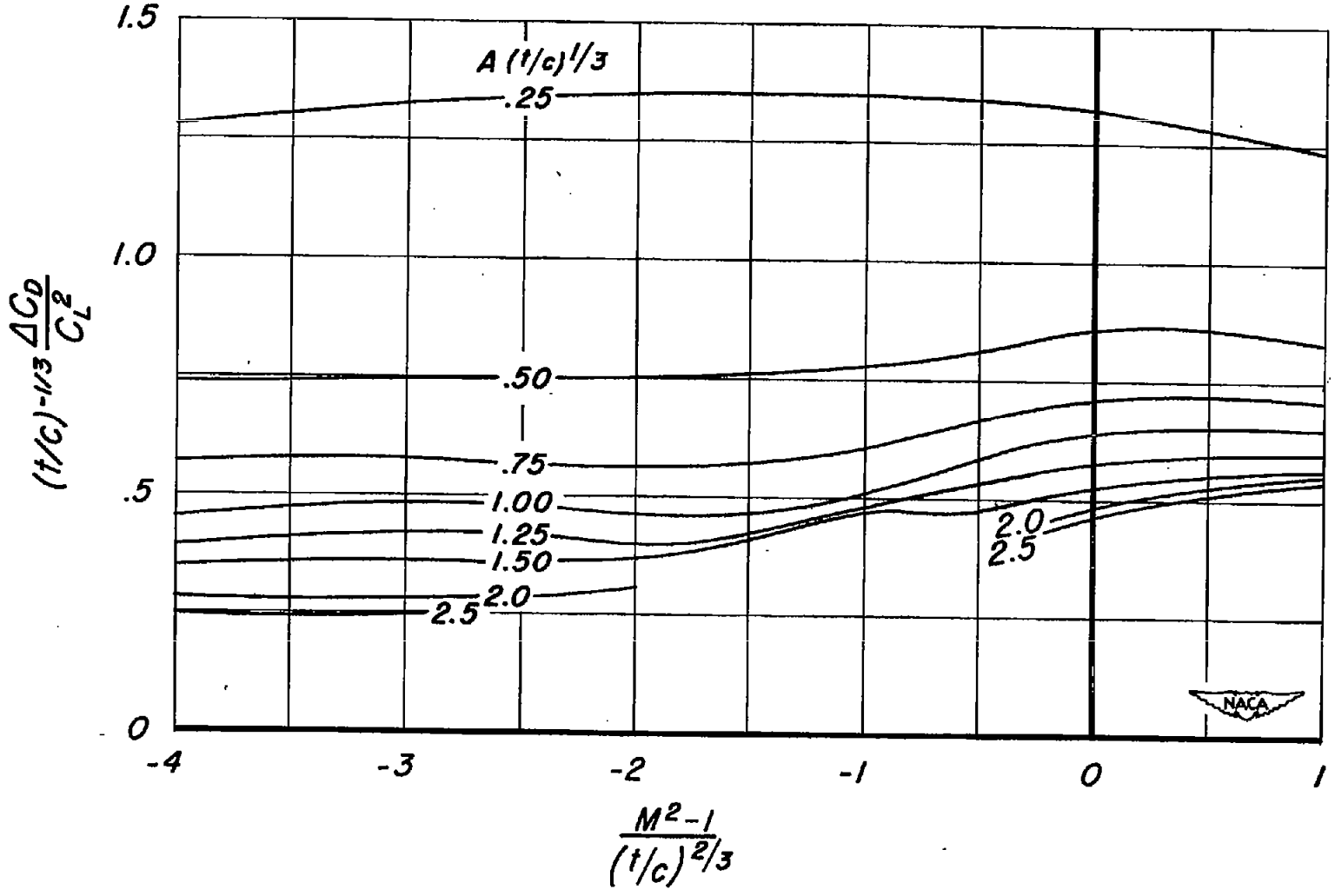


Figure 18.—Summary curves for $(t/c)^{-1/3} \frac{\Delta C_D}{C_L^2}$

CONFIDENTIAL

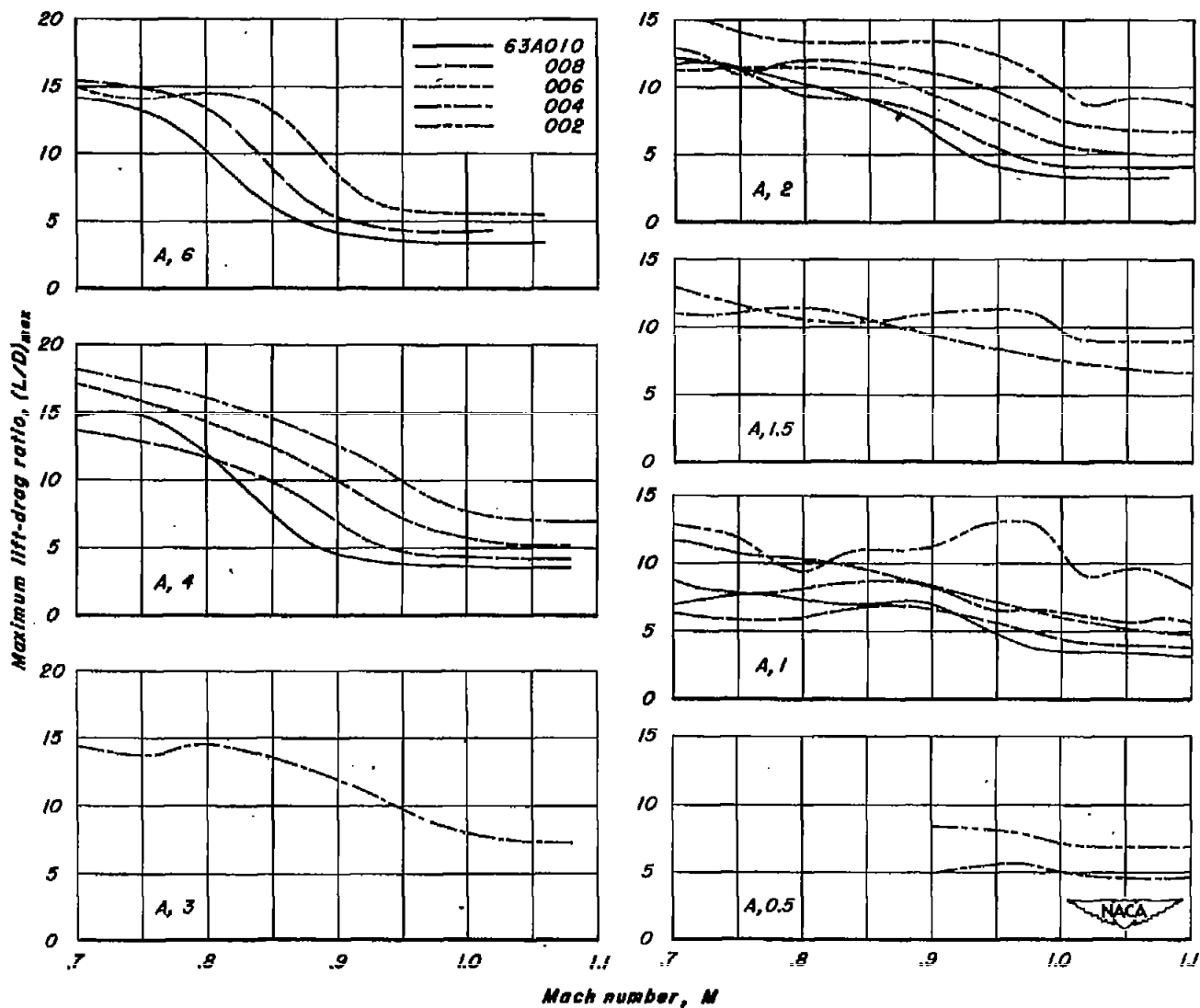


Figure 19.- The variation of maximum lift-drag ratio with Mach number.

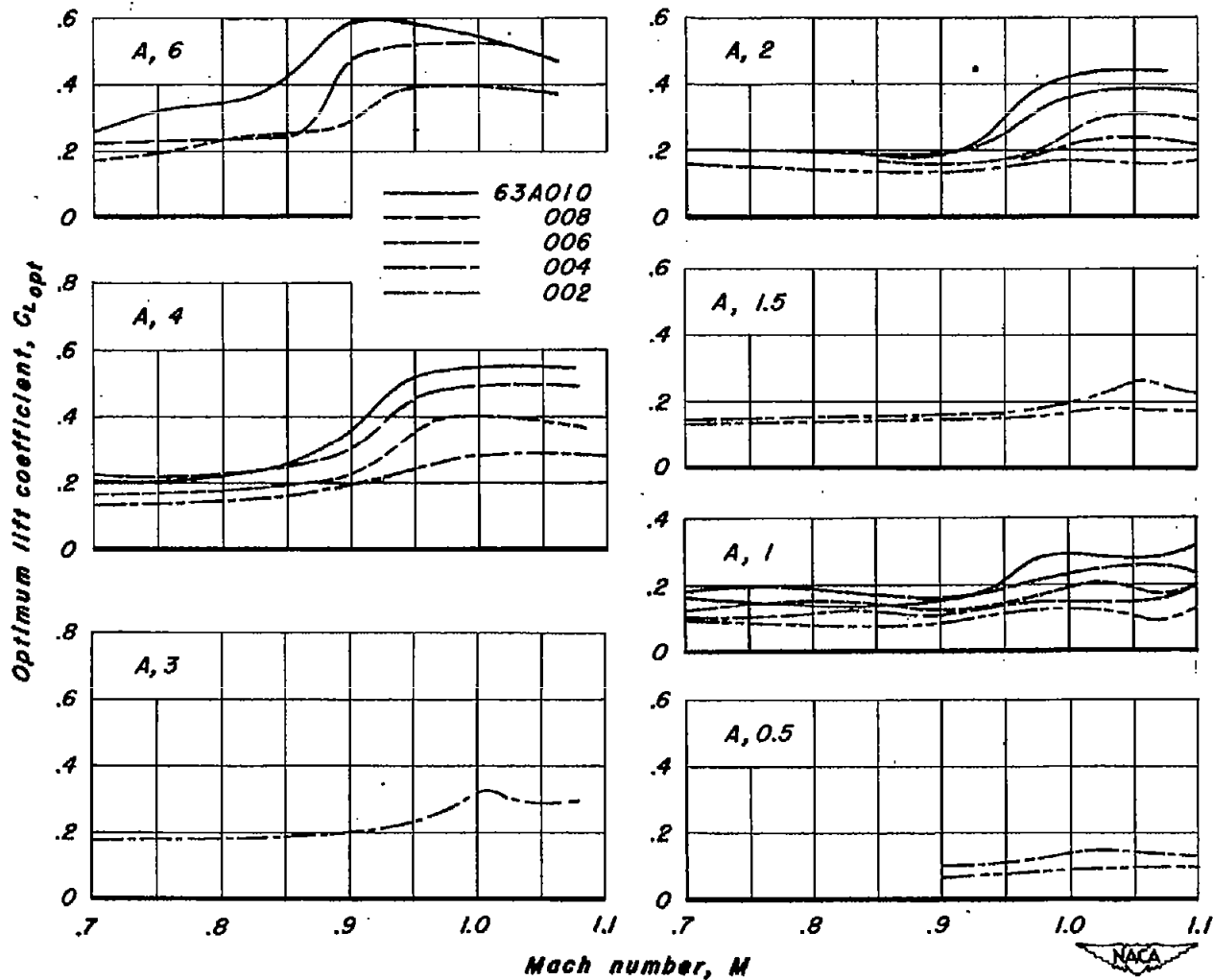


Figure 20.- The variation of lift coefficient for maximum lift-drag ratio with Mach number.

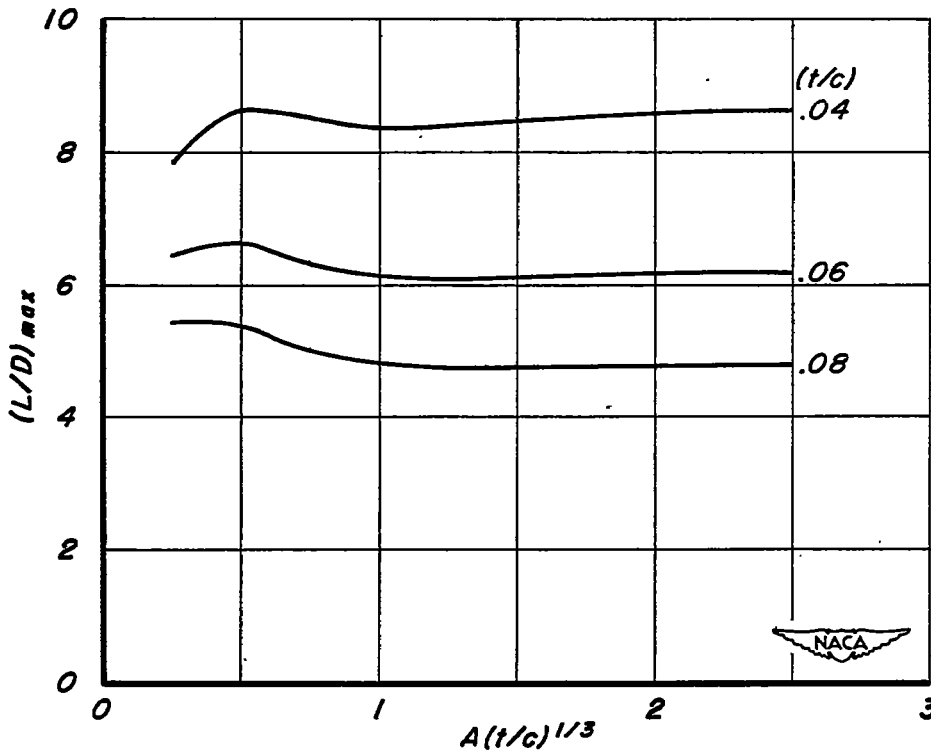
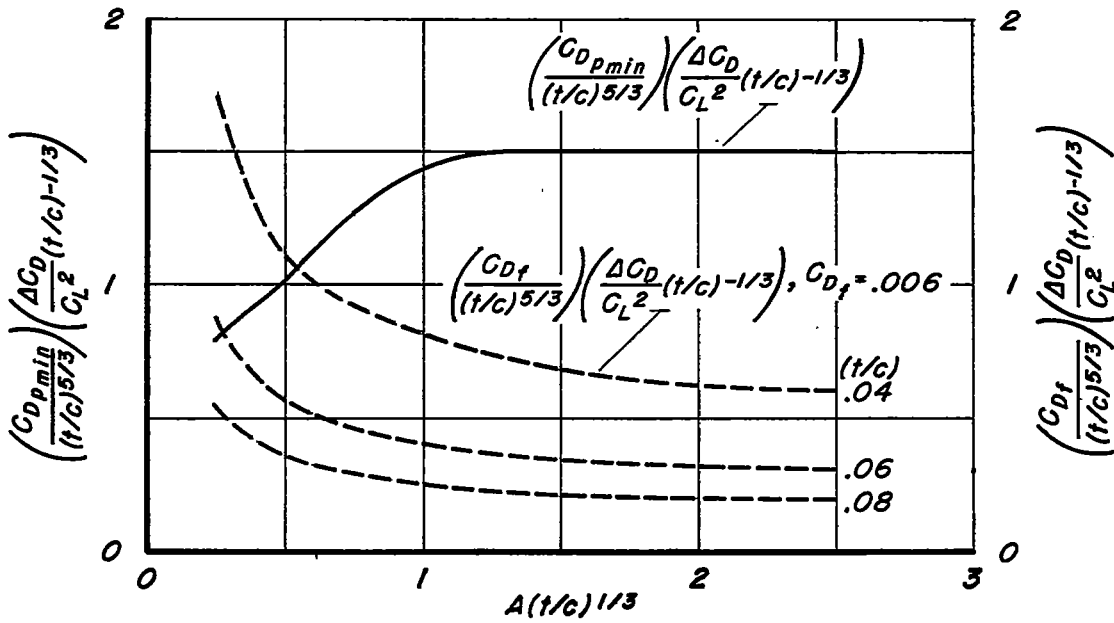


Figure 21.- Maximum lift-drag ratios at sonic speed.

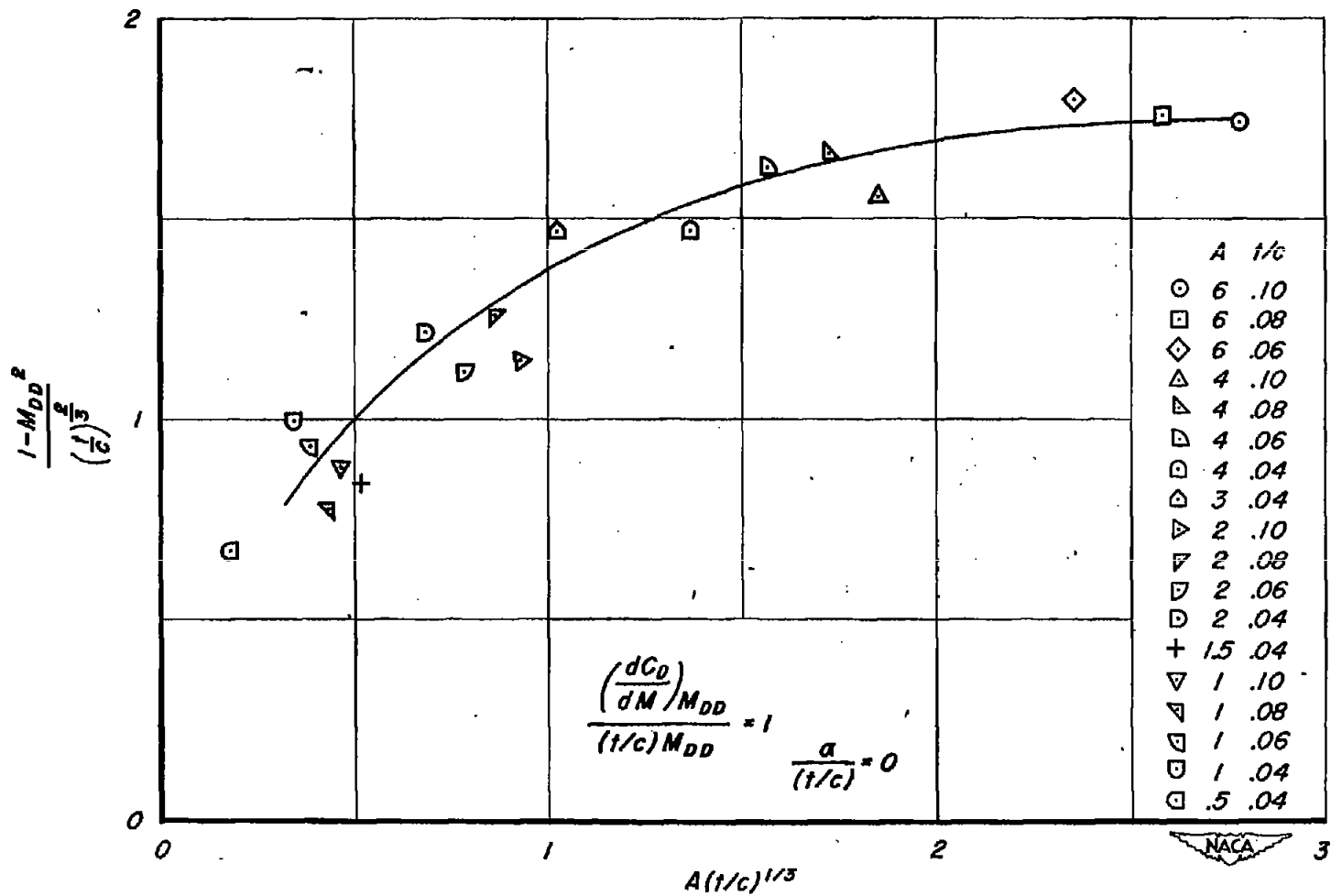


Figure 22: Variation of the drag-divergence Mach number parameter, $\frac{1-M_{DD}^2}{(t/c)^{2/3}}$, with $A(t/c)^{1/3}$.